

Chapter 3: Partially Nonlinear Single-Index Predictive Model

1 Introduction

Background

Forecasting of stock return is central to making investment decisions. Development of models and methodologies for selecting a good predictive model and constructing reliable forecast have been an active area of research. Linear models were widely used in early studies (Campbell and Shiller (1988), Fama (1990), and Pesaran and Timmermann (1995)), but as most of the predictors used to predict stock return (for example, some macroeconomic variables) are non-stationary, linear models will suffer from the problem of spurious regression. Therefore, in the past two decades, nonlinear and non-stationary time series have attracted much attention and have been studied intensively

In this chapter, we propose a new class of nonlinear time series models - partially nonlinear single-index models of the form:

$$y_t = \beta_0' z_t + f(x_{t-1}' \theta_0; \gamma_0) + e_t, \quad t = 2, \dots, T, \quad (1.1)$$

where $z_t = (y_{t-1}, \dots, y_{t-p}, w_{t-1}')'$, in which w_{t-1} is a vector of stationary predictors, $g(\cdot, \cdot)$ is a known univariate nonlinear function, x_{t-1} is a d -dimensional integrated process of order one, θ_0 is a d -dimensional unknown true parameter vector that lies in the parameter set Θ , γ_0 is a m -dimensional unknown true parameter vector that lies in the parameter set Γ and e_t is a martingale difference process. The parameter sets Θ and Γ are assumed to be compact and convex subsets of \mathbb{R}^d and \mathbb{R}^m respectively. In order to ensure that θ_0 is uniquely identifiable, we will need to impose $\theta_0' \theta_0 = 1$.

This model combines linear components with a nonlinear single-index component, which can capture both linear and nonlinear relationship between dependent variable and predictors. This study aims to use the Monte Carlo simulation method to investigate the finite sample properties of the estimators. There will also be an empirical analysis using [Welch and Goyal \(2008\)](#) dataset, to compare the out-of-sample predictability of stock returns with commonly used benchmark models.

Literature Review

Since real world data always display different characteristics, simple linear models are not adequate in doing modelling and prediction. In recent decades, there is a considerable practical and theoretical effort being channelled into nonlinear and nonstationary time series (see for example, [Park and Phillips \(2001\)](#), [Park \(2002\)](#) and [Gao et al. \(2009\)](#)).

In the early years, [Jennrich \(1969\)](#) and [Wu \(1981\)](#) establish the asymptotic theories for non-linear least square estimators. [Wooldridge \(1994\)](#) and [Andrews and McDermott \(1995\)](#) then develop the theory for trending processes. [Park and Phillips \(2001\)](#) and [Chang et al. \(2001\)](#) then extend the theories to include integrated time series. They propose a parametric additive model and estimate the parameters using nonlinear least square method. However, the nonlinear regressions they consider can only include singular predictor.

In the case of multiple predictors, [Chang and Park \(2003\)](#) proposes index models driven by integrated time series of the form:

$$y_t = G(v + x'_t\beta) + u_t$$

where x_t is an m-dimensional integrated process of order one, u_t is a stationary error. This model combines the multiple predictors in to a single-index structure $x'_t\beta$. It is a parametric model since $G(v + x'_t\beta)$ is known, and all the estimators are estimated by nonlinear least square method.

But as parametric models may suffer from the misspecification problem, some non-parametric models have been studied intensively and different estimation method has been proposed, such as kernel estimation ([Xia and Härdle \(2006\)](#), [Ma and Song \(2015\)](#), [Birke et al. \(2017\)](#)), series-based method ([Chen \(2007\)](#) for review), spline method ([Yu](#)

and Ruppert (2002)) and Hermite polynomials (see for example, Dong et al. (2015)).

Meanwhile, to make the nonparametric models more flexible, semiparametric models involving both parametric and nonparametric components have been widely studied in the literature, such as by Gao (2007). As the non-parametric part can describe the nonlinear relationship among variables, studies normally use linear component as the parametric part (the so called partially linear model). In the time series literature, partially linear model with single-index structure have also attracted attention in recent years. For example, Dong et al. (2016) propose a partially linear single-index model of the form:

$$y_t = \beta_0' x_t + g(\theta_0' x_t) + e_t \quad (1.2)$$

where y_t is a scalar process, $g(\cdot)$ is an unknown nonlinear integrable function (the link function), x_t is a d-dimensional integrated process. This model is an extension of parametric linear models and at the same time, a compromise between fully parametric and fully nonparametric models.

But model (1.2) only includes integrated processes, while in economic and financial studies, the regressors are a mixture of stationary and non-stationary variables. For example, some popular predictors used in stock return prediction are non-stationary, such as dividend-price ratio (Fama and French (1989), Cochrane (2008), and Lettau and Van Nieuwerburgh (2008)), earnings-price-ratio (Campbell and Shiller (1988)) and book-to-market ratio (Kothari and Shanken (1997) and Pontiff and Schall (1998)). While some stationary predictors are also proved to be important, such as the regression residuals in the study of Lettau and Ludvigson (2001).

In addition, models like (1.2) did not include lag variable $y_{t-1}, y_{t-2}, \dots, y_{t-p}$. It may limit their applications to time series modelling because key macroeconomic/financial variables, such as the growth rate of GDP and the rate of unemployment are typically auto-correlated. Failing to account for this auto-correlation will lead to serially correlated residuals.

Therefore, we propose model (1.1) to include time series with different characteristics. In our model:

$$y_t = \beta_0' z_t + f(x_{t-1}' \theta_0; \gamma_0) + e_t, \quad t = 2, \dots, T,$$

z_t contains all the stationary variables. In stock return predictability case, y_{t-1} is included

in z_t since stock return is stationary. x_t in the single-index component includes non-stationary variables and in our study, we consider non-stationary predictors with co-integrated structure (see for example, [Zhou et al. \(2018\)](#)).

For the parametric function $f(\cdot)$, we adopt some commonly used nonlinear functional forms. There is a considerable theoretical effort being put into the theoretical study of nonlinear models. [Park and Phillips \(1999\)](#), [Park and Phillips \(2000\)](#), [Park and Phillips \(2001\)](#) develop asymptotic theory for nonlinear models with single predictor. [Chang et al. \(2001\)](#) and [Chang and Park \(2003\)](#) extend the theory to include multiple predictors. Non-linear relationship has also been considered in forecasting financial and macroeconomic series in empirical studies. [Qi \(1999\)](#) adopts a neural network model with 9 financial and economic variables. [Lettau and Van Nieuwerburgh \(2008\)](#) provide strong in-sample evidence for regime shifts in the long-term mean of the dividend-price ratio.

Building on this growing literature, this chapter focuses on assessing the stock return predictability using the partially nonlinear models. The motivations of this study are as follows. Stock return has been proved to be predictable (see for example, [Fama \(1981\)](#), [Fama \(1990\)](#), [Campbell et al. \(2004\)](#) and [Campbell and Yogo \(2006\)](#)), but [Welch and Goyal \(2008\)](#) find that the predictability only holds in in-sample prediction, not out-of-sample. Therefore, the first motivation of this study is to investigate whether our partially nonlinear models can perform better both in-sample and out-of-sample. Moreover, we have considered a pure nonlinear model in our previous study. in this chapter, we are motivated to check whether including lagged dependent variables would, in fact, improve forecasts of y_t relative to using only nonlinear single-index component, $f(x'_{t-1}\theta_0; \gamma_0)$.

Furthermore, in the study of [Welch and Goyal \(2008\)](#), they only use historical average as the benchmark model. In our study, we will compare our models against different benchmark models, including auto-regressive models, linear models and nonlinear models. By doing so, we can investigate that after combining linearity with nonlinearities, whether our model can outperform pure linear or nonlinear models. Our model may also be useful in cases where there are additional stationary predictors, w_{t-1} , for which the linear specification fits the data better than the nonlinear specification.

To estimate model (1.1), we propose a novel 3-step estimation method in which β will have a closed form solution while θ and γ can be estimated by the method of nonlinear

least squares or constrained nonlinear least squares. As we need to use an iterative procedure to apply the nonlinear least square estimation, we design a 2-step technique using Taylor series expansions to help us choose initial values.

The findings of this chapter are summarized as follows. First, from the Monte Carlo simulation, we find that the constrained nonlinear least square estimators have good finite sample performances and they perform better than the estimator without constraint. Second, we find that the Taylor initial values help further improve the performance. Third, in the empirical study, we find both in-sample and out-of-sample evidence that the partially nonlinear model we propose have a better performance than the historical average model. Finally, we also find that model (1.1) provides a better out-of-sample performance than other benchmark models.

This chapter is organized as follows. Section 2 introduces the partially nonlinear single-index predictive model and proposes a 3-step estimation method. To improve the performance of the model, this section also introduces constraint and truncation conditions in addition to the normal nonlinear least square. Section 3 examines the finite-sample properties of the normal nonlinear least square estimators (NLS estimators hereafter) and the constrained nonlinear least square estimators (CLS estimators hereafter) using Monte Carlo evaluation. The discussion includes models with different nonlinear functional part and considers both co-integrated and non-cointegrated cases. Section 4 applies the partially nonlinear models to stock return predictability and investigate both in-sample and out-of-sample performances of the models. Section 5 concludes.

2 Model and Methodology

2.1 Estimation Method

Since in our case, $f(x'_{t-1}\theta_0; \gamma_0)$ is known, model (1.1) can be estimated by using a nonlinear least square method. Let $L(\beta, \theta, \gamma) = \sum_{t=1}^T \left(y_t - \beta' z_t - f(x'_{t-1}\theta; \gamma) \right)^2$, and hence we have the following gradient functions:

$$\begin{aligned}
\frac{\partial L(\beta, \theta, \gamma)}{\partial \beta} &= -2 \sum_{t=1}^T z'_t \left(y_t - \beta' z_t - f(x'_{t-1} \theta; \gamma) \right) \\
\frac{\partial L(\beta, \theta, \gamma)}{\partial \theta} &= -2 \sum_{t=1}^T \left(y_t - \beta' z_t - f(x'_{t-1} \theta; \gamma) \right) \frac{\partial g(x'_{t-1} \theta; \gamma)}{\partial \theta} \\
\frac{\partial L(\beta, \theta, \gamma)}{\partial \gamma} &= -2 \sum_{t=1}^T \left(y_t - \beta' z_t - f(x'_{t-1} \theta; \gamma) \right) \frac{\partial g(x'_{t-1} \theta; \gamma)}{\partial \gamma}
\end{aligned} \tag{2.1}$$

The minimum value of $L(\beta, \theta, \gamma)$ occurs when the above gradient functions equals to 0. Notice that these score functions $\frac{\partial L(\beta, \theta, \gamma)}{\partial \theta}$ and $\frac{\partial L(\beta, \theta, \gamma)}{\partial \gamma}$ are nonlinear functions of both the variables and the parameters, and so they do not have closed form solutions. To estimate the parameters, we need to include an iterative procedure and obtain optimal values by using gradient descent algorithms. However, recognizing that this score function $\frac{\partial L(\beta, \theta, \gamma)}{\partial \beta}$ is linear in the parameter β , we introduce a novel 3-step approach for estimation in order to reduce the computational burden.

Step 1: set $\frac{\partial L(\beta, \theta, \gamma)}{\partial \beta} = 0$ and solve the first equation in (2.1) to obtain $\tilde{\beta}$:

$$\tilde{\beta} = \left(\sum_{t=1}^T z_t z'_t \right)^{-1} \sum_{t=1}^T \left(y_t - f(x'_{t-1} \theta; \gamma) \right) z_t \tag{2.2}$$

In other words, $\tilde{\beta}$ is of a linear form by OLS expression. Thus model (1.1) can be approximated by:

$$y_t = \tilde{\beta}' z_t + f(x'_{t-1} \theta; \gamma) + e_t,$$

Substitute $\tilde{\beta}$ in (2.2) and rearrange the equation above, we can get:

$$y_t - \left(\left(\sum_{t=1}^T z_t z'_t \right)^{-1} \sum_{t=1}^T y_t z_t \right)' z_t = f(x'_{t-1} \theta; \gamma) - z'_t \left(\sum_{t=1}^T z_t z'_t \right)^{-1} \sum_{t=1}^T f(x'_{t-1} \theta; \gamma) z_t + e_t.$$

Let

$$\begin{aligned}
\tilde{y} &= y_t - z'_t \left(\sum_{t=1}^T z_t z'_t \right)^{-1} \sum_{t=1}^T y_t z_t, \\
\tilde{g}(x'_{t-1} \theta; \gamma) &= f(x'_{t-1} \theta; \gamma) - z'_t \left(\sum_{t=1}^T z_t z'_t \right)^{-1} \sum_{t=1}^T f(x'_{t-1} \theta; \gamma) z_t
\end{aligned}$$

Then we have an approximate model of the form:

$$\tilde{y} = \tilde{g}(x'_{t-1}\theta; \gamma) + e_t. \quad (2.3)$$

Step 2: estimate $(\hat{\theta}, \hat{\gamma})$ using nonlinear least square(NLS) method. Define the sum of least squares $Q_T(\theta, \gamma)$ as:

$$Q_T(\theta, \gamma) = \sum_{t=1}^T \left(\tilde{y}_t - \tilde{g}(x'_{t-1}\theta, \gamma) \right)^2$$

over $(\theta, \gamma) \in (\Theta, \Gamma)$. The estimated $(\hat{\theta}, \hat{\gamma})$ is given by:

$$(\hat{\theta}, \hat{\gamma}) = \arg \min_{\theta \in \Theta, \gamma \in \Gamma} Q_T(\theta, \gamma),$$

which can be solved using an iterative procedure since there is no closed form solutions.

Step 3: As $\hat{\theta}$ and $\hat{\gamma}$ have been estimated, we can substitute them back to (2.2) and get the estimate of β :

$$\hat{\beta} = \left(\sum_{t=1}^T z_t z'_t \right)^{-1} \sum_{t=1}^T \left(y_t - f(x'_{t-1}\hat{\theta}; \hat{\gamma}) \right) z_t.$$

In the 3-step procedure above, we have obtained the NLS estimators $(\hat{\theta}, \hat{\gamma}, \hat{\beta})$. In order to improve finite sample properties of the estimators, we impose a truncation condition $I(\|x_{t-1}\| \leq M_T)$ on x_{t-1} and an identification condition on coefficient vector θ . We then define the modified sum-of-squared errors by:

$$Q_{T,M}(\theta, \gamma) = \sum_{t=1}^T \left(y_t - f(x'_{t-1}\theta, \gamma) \right)^2 I(\|x_{t-1}\| \leq M_T) + \lambda (\|\theta\|^2 - 1), \quad (2.4)$$

where $I(\cdot)$ denotes the indicator function, λ is a Lagrange multiplier and $\|\cdot\|$ is the Euclidean norm. In equation (2.4), the truncation condition $I(\|x_{t-1}\| \leq M_T)$ discards observations whose Euclidean norm is bigger than M_T . Similar condition has been considered by Li et al. (2016) and Ling (2007). M_T is a positive and increasing sequence satisfying $M_T \rightarrow \infty$ as $T \rightarrow \infty$. Following Li et al. (2016), we choose $M_T = C_\alpha n^{1-\beta}$ with $\beta = 1/2$ and $C_\alpha = 1$. Therefore, $M_T = \sqrt{T}$ in our study.

Then we can start with step 1 above to rearrange the equations and the constrained least squares (denoted CLS) estimators $\bar{\theta}$ and $\bar{\gamma}$ can be obtained by minimizing $Q_{T,M}(\theta, \gamma)$ over $\theta \in \Theta$ and $\gamma \in \Gamma$ such that the two restrictions hold; that is:

$$(\bar{\theta}, \bar{\gamma}) = \arg \min_{\theta \in \Theta, \gamma \in \Gamma, \|\theta\|^2=1} Q_{T,M}(\theta, \gamma).$$

And the CLS estimator of β can be written as:

$$\bar{\beta} = \left(\sum_{t=1}^T z_t z_t' \right)^{-1} \sum_{t=1}^T \left(y_t - f(x_{t-1}' \bar{\theta}; \bar{\gamma}) \right) z_t.$$

2.2 Nonlinear Function: $f(x_{t-1}' \theta_0, \gamma_0)$

In the partially nonlinear model (1.1), we consider different forms of $f(x_{t-1}' \theta_0, \gamma_0)$ to include various types of nonlinearities. The first group of nonlinear functions we consider is the trigonometric functions:

$$\begin{aligned} \sin : f_1(u_{t-1}, \gamma_1) &= \sin(u_{t-1} + \gamma_1), \\ \cos : f_2(u_{t-1}, \gamma_2) &= \cos(u_{t-1} + \gamma_2), \\ \sin_scaled : f_3(u_{t-1}, \gamma_3, \gamma_4) &= \sin(\gamma_3 u_{t-1} + \gamma_4), \\ \cos_scaled : f_4(u_{t-1}, \gamma_5, \gamma_6) &= \cos(\gamma_5 u_{t-1} + \gamma_6), \end{aligned}$$

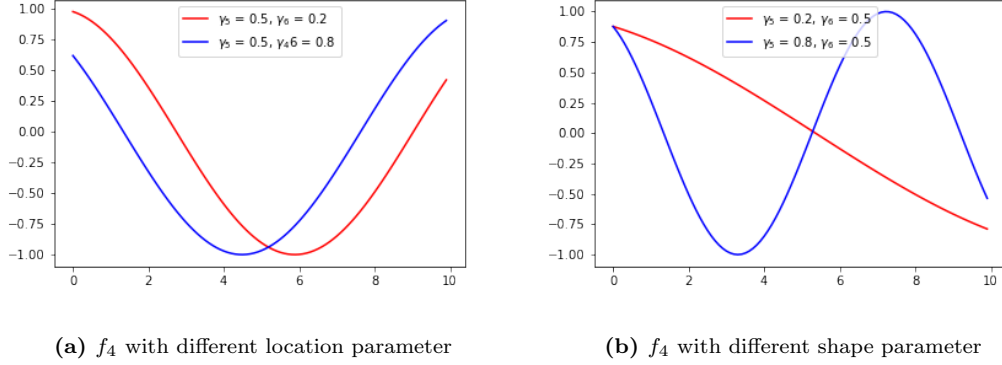
where $u_{t-1} = x_{t-1}' \theta_0$. Among the above 4 trigonometric functions, $f_1(x_{t-1}' \theta_0, \gamma_0)$ and $f_2(x_{t-1}' \theta_0, \gamma_0)$ can be regarded as special cases of $f_3(x_{t-1}' \theta_0, \gamma_0)$ and $f_4(x_{t-1}' \theta_0, \gamma_0)$ with γ_3 and γ_5 equal to 1.

Parameters $\gamma_1, \gamma_2, \gamma_4$ and γ_6 decide the position of the functions (the location parameter). As shown in picture (1a), the two curves have the same shape but the red curve is to the right of the blue one. Parameters γ_3 and γ_5 decide the shape of the functions, a bigger value will make the shape more compressed while a smaller value will make it more stretched (the shape parameter). The effect of the shape parameters can be seen in picture (1b). The blue curve shows almost one period of a cosine function but the red curve shows less than a quarter.

In addition, we also consider two exponential functions:

$$\exp_shift : f_5(u_{t-1}, \gamma_7, \gamma_8) = 1 - e^{-\gamma_7(u_{t-1} - \gamma_8)^2}$$

Figure 1: Plots for Trigonometric Functions

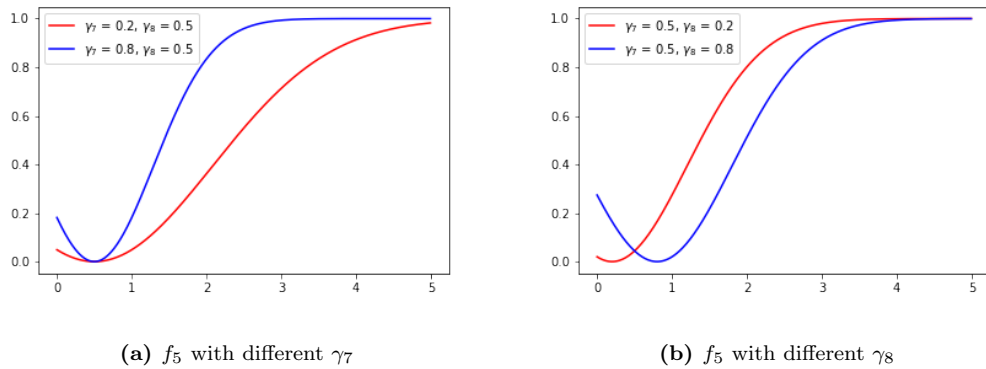


$$\exp : f_6(u_{t-1}, \gamma_9, \gamma_{10}) = \gamma_9 e^{-\gamma_{10} u_{t-1}^2},$$

where $\gamma_7, \gamma_{10} \in (0, \infty)$. The two exponential functions are bounded: $f_5(x'_{t-1}\theta_0, \gamma_0)$ lies in $(0, 1)$ and $f_6(x'_{t-1}\theta_0, \gamma_0)$ lies in $(0, \gamma_9)$.

Figure 2 and 3 present the plots of $f_5(x'_{t-1}\theta_0, \gamma_0)$ and $f_6(x'_{t-1}\theta_0, \gamma_0)$. Even though both f_5 and f_6 are exponential functions, they have very different shapes. f_5 is an increasing function while f_6 is a decreasing function. We can see that γ_7 changes the steepness of $f_5(x'_{t-1}\theta_0, \gamma_0)$ (figure 2a) and γ_8 changes its position (figure 2b). And for $f_6(x'_{t-1}\theta_0, \gamma_0)$, γ_9 acts as the upper bound for the function and changes its position (figure 3a), while γ_{10} changes its steepness (figure 3b).

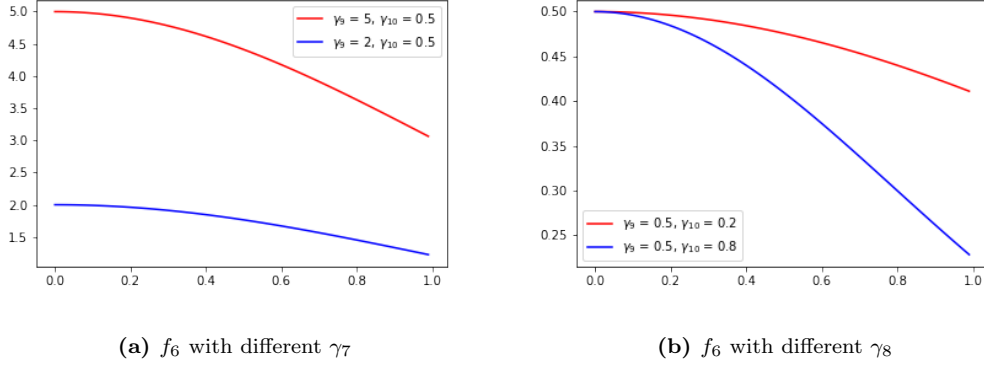
Figure 2: $f_5(x'_{t-1}\theta_0, \gamma_0)$ with different γ



In addition, we also consider a quadratic polynomial function:

$$\text{Polynomial} : f_7(u_{t-1}, \gamma_{11}, \gamma_{12}, \gamma_{13}) = \gamma_{11} + \gamma_{12}u_{t-1} + \gamma_{13}u_{t-1}^2$$

Figure 3: $f_6(x'_{t-1}\theta_0, \gamma_0)$ with different γ



It is a parabola where γ_{11} decides the y-intercept and γ_{13} reflects the parabola's wideness.

The nonlinear functional forms we consider have included the bounded functions (the exponential functions), bounded periodic functions (trigonometric functions), and the unbounded function (polynomial function).

2.3 Initial Values

As the gradient functions (2.1) do not have a closed form solution, we will use an iterative procedure, which requires initial values, to estimate the model. Most studies use 0 or true values as the initial values to start the procedure. Normally, true values provide the quickest and best convergence, but they are not known in empirical studies. Therefore, we want to find values that are close to the optimal values to get a better convergence.

To do so, we can approximate the nonlinear component in model (??) by a linear model using Taylor series expansion. Since both γ and θ are unknown parameters, we need to calculate θ (denoted by θ_0) first to obtain u_{t-1}^\wedge . As we only consider cointegrated x_1 and x_2 in this chapter, we can first estimate the following regression to get the cointegration vector $(1, -\hat{\eta})$:

$$x_1 = \eta x_2 + e_t, \quad e_t \sim i.i.d.N(0, 1), \quad t = 2, \dots, T$$

Then θ_0 is given by normalizing the cointegration vector $(1, -\hat{\eta})$:

$$\theta_0 = \left(\frac{1}{\sqrt{1 + \hat{\eta}^2}}, -\frac{\hat{\eta}}{\sqrt{1 + \hat{\eta}^2}} \right)$$

which satisfies the constrain that $\|\theta_0\| = 1$. Then the single-index can be calculated as

$$\hat{u}_{t-1} = x'_{t-1}\theta_0.$$

Since \hat{u}_{t-1} has been estimated, we can apply Taylor series expansion to approximate the nonlinear part $f(\hat{u}_{t-1}, \gamma_0)$. For the two sine functions: $f_1(u_{t-1}, \gamma_0) = \sin(u_{t-1} + \gamma_1)$ and $f_3(\gamma_3 u_{t-1}, \gamma_4) = \sin(\gamma_3 u_{t-1} + \gamma_4)$, we can use their first order Taylor series expansions and substitute f_1 and f_3 by:

$$\tilde{f}_1 = (\hat{u}_{t-1} + \gamma_1)$$

$$\tilde{f}_3 = (\gamma_3 \hat{u}_{t-1} + \gamma_4)$$

Then for the two cosine functions $f_2(u_{t-1}, \gamma_2) = \cos(u_{t-1} + \gamma_2)$ and $f_4(\gamma_5 u_{t-1} + \gamma_6) = \cos(\gamma_5 u_{t-1} + \gamma_6)$, we approximate them using their second-order Taylor series expansions:

$$\tilde{f}_2 = 1 - (\hat{u}_{t-1} + \gamma_2)^2$$

$$\tilde{f}_4 = 1 - (\gamma_5 \hat{u}_{t-1} + \gamma_6)^2$$

Similarly, the two exponential functions $f_5(u_{t-1}, \gamma_7, \gamma_8) = 1 - e^{-\gamma_7(u_{t-1} - \gamma_8)^2}$ and $f_6(u_{t-1}, \gamma_9, \gamma_{10}) = \gamma_9 e^{-\gamma_{10} u_{t-1}^2}$ can also be approximated by their first and second order Taylor series expansions respectively:

$$\tilde{f}_5 = \gamma_7(\hat{u}_{t-1} - \gamma_8)^2$$

$$\tilde{f}_6 = \gamma_9(1 - \gamma_{10} \hat{u}_{t-1}^2 + \frac{\gamma_{10}^2 \hat{u}_{t-1}^4}{2})$$

And for functional 7, the polynomial function, it is already a linear function when the single-index is known.

Therefore, we can substitute the nonlinear part f_1 to f_6 in model (1.1) by \tilde{f}_1 to \tilde{f}_6 above and the initial values of (β, γ) for different functional forms can be calculated by estimating the following linear regressions:

$$y_t = \gamma_1 + \hat{u}_{t-1} + \beta_1 y_{t-1} + \beta_2 w_{t-1} + e_t$$

$$y_t = \gamma_2 + \hat{u}_{t-1} + \beta_1 y_{t-1} + \beta_2 w_{t-1} + e_t$$

$$y_t = \gamma_4 + \gamma_3 \hat{u}_{t-1} + \beta_1 y_{t-1} + \beta_2 w_{t-1} + e_t$$

$$y_t = \gamma_6 + \gamma_5 \hat{u}_{t-1} + \beta_1 y_{t-1} + \beta_2 w_{t-1} + e_t$$

$$y_t = \gamma_7 \hat{u}_{t-1}^2 - 2\gamma_7 \gamma_8 \hat{u}_{t-1} + \gamma_7 \gamma_8^2 + \beta_1 y_{t-1} + \beta_2 w_{t-1} + e_t$$

$$y_t = \gamma_9(1 - \gamma_{10} \hat{u}_{t-1}^2 + \frac{\gamma_{10}^2 \hat{u}_{t-1}^4}{2}) + \beta_1 y_{t-1} + \beta_2 w_{t-1} + e_t$$

$$y_t = \gamma_{11} + \gamma_{12}\hat{u}_{t-1} + \gamma_{13}\hat{u}_{t-1}^2 + \beta_1 y_{t-1} + \beta_2 w_{t-1} + e_t$$

where $\hat{u}_{t-1} = x'_{t-1}\theta_0$ and $e_t \sim i.i.d.N(0, 1)$, $t = 2, \dots, T$.

Together with θ_0 , we have calculated the initial values $(\theta_0, \beta_0, \gamma_0)$ for the iterative procedure. In the section below, we can see that when compared with other initial values, the Taylor initial values can improve the finite sample performance significantly.

3 Monte Carlo Simulation

3.1 Data Generation Processes

We investigate the finite sample properties of the NLS and the proposed CLS estimators for partially nonlinear model in multivariate co-integrated and non-cointegrated settings. The predictors x_{t-1} is a 2-vector integrated time series. Data are generated on the following models:

$$y_t = \beta_{1,0}y_{t-1} + \beta_{2,0}w_{t-1} + f(x'_{t-1}\theta_0, \gamma_0) + e_t, \quad e_t \sim i.i.d.N(0, 1), \quad t = 2, \dots, T,$$

with

$$\begin{aligned} w_t &= 0.8 * w_{t-1} + s_t, \quad s_t \sim i.i.d.N(0, 1), \\ x_t &= x_{t-1} + v_t \end{aligned} \tag{3.1}$$

In terms of x_t , we consider both cointegrated x_t and non-cointegrated x_t in this simulation study. When x_t is not cointegrated, v_t in (3.1) is given by:

$$v_t = \begin{pmatrix} v_{1,t} \\ v_{2,t} \end{pmatrix} \sim N \left(\begin{pmatrix} 0 \\ 0 \end{pmatrix}, \begin{pmatrix} 1 & 0.5 \\ 0.5 & 1 \end{pmatrix} \right)$$

To generate the co-integrated x_t , we follow a vector integrated process driven by an MA(1) innovations and construct v_t in (3.1) as:

$$v_t = \epsilon_t + C\epsilon_{t-1},$$

$$\text{where } \epsilon_t \sim i.i.d.N \left(\begin{pmatrix} 0 \\ 0 \end{pmatrix}, \begin{pmatrix} 1 & 0.5 \\ 0.5 & 1 \end{pmatrix} \right) \text{ and } C = \begin{pmatrix} -1 & 4/3 \\ 0 & 0 \end{pmatrix}.$$

In the data generation process, we consider true parameter values $\hat{\theta}_0 = (0.8, -0.6)'$, $\beta_{1,0} = 0.5$, $\beta_{2,0} = 1.0$, and $\gamma_0 = (0.2, 0.3, 0.5)$. The vector length of γ_0 varies depending on the nonlinear form $f(x'_{t-1}\theta_0, \gamma_0)$ we select.

In our simulation study, we consider sample sizes $T = 100, 500, 1000$, replication time $M = 5000$ and calculate the following statistics:

$$\text{bias}(\hat{\alpha}_i) = \bar{\alpha}_i - \alpha_{i,0},$$

where $\bar{\alpha}_i = M^{-1} \sum_{r=1}^M \hat{\alpha}_i^{(r)}$; and the standard deviation:

$$\text{std}(\hat{\alpha}_i) = \sqrt{M^{-1} \sum_{r=1}^M \left(\hat{\alpha}_i^{(r)} - \bar{\alpha}_i \right)^2}.$$

Since $\hat{\alpha}_1$ and $\hat{\alpha}_2$ are correlated, we also calculate a type of estimated covariance of the form:

$$\sigma_{ij} = \frac{1}{M} \sum_{r=1}^M \left(\hat{\alpha}_i^{(r)} - \bar{\alpha}_i \right) \left(\hat{\alpha}_j^{(r)} - \bar{\alpha}_j \right), \quad \text{cov}(\hat{\alpha}) \sqrt{\sum_{i=1}^2 \sum_{j=1}^2 \sigma_{ij}^2}.$$

where $\hat{\alpha}^{(r)}$ denote the r -th replication of the estimate. Following the above definitions, we then calculate biases, standard deviations and covariance for θ , β and γ .

3.2 Simulation Results

In this part, we first present results for different initial values and conclude that the Taylor initial values have better performance. We then show the simulation results for cointegrated and non-cointegrated x_1, x_2 using the Taylor initial values.

Compare Different Initial Values

We use the polynomial function as an example to compare different initial values (other functional forms have similar performances). Table 1 shows the simulation results for the partially nonlinear model with polynomial function $f(u_{t-1}, \gamma)$:

$$y_t = \gamma_{11} + \gamma_{12}u_{t-1} + \gamma_{13}u_{t-1}^2 + \beta_1 y_{t-1} + \beta_2 w_{t-1} + e_t$$

where $u_{t-1} = x'_{t-1}\theta$ and $e_t \sim i.i.d.N(0, 1)$, $t = 2, \dots, T$. From the table, we can see that the CLS estimators achieve the best convergence when using true values to start the

iterative procedure. The biases and standard deviations of the estimators are at very low levels even when sample size $T = 100$. And it continues to decrease when sample size increases.

But when using 0 as initial values, the simulation performance is much worse. Take sample size $T = 500$ and θ_1 as an example, the standard deviation of θ_1 is 0.2855, while when using true values, the standard deviation of θ_1 is 0.00029. It also shows that the convergence become worse when initial values equal to 0. For example, the bias of θ_1 is 0.12214 when $T = 100$, and it is 0.15770 when $T = 1000$.

Even though the true values provide much better results, it is not realistic to use them for empirical studies. Therefore, we calculate the Taylor initial values following the procedure in previous section to estimate our partially nonlinear models. As the Taylor initial values we obtain should be relatively close to the true values, we expect the simulation results to be better than using random initial values.

We can see from the first panel in table 1 that when using the Taylor initial values, the standard deviation of θ_1 has decreased from 0.2855 (when initial values equals to 0) to 0.0004. It also shows a good convergence, where the biases and standard deviations both decreases when then sample size increases. Take the covariance of γ : $\text{cov}(\gamma)$ as an example, the covariance drops from 0.01029 when $T = 100$, to 0.00339 when $T = 1000$.

Therefore, compare with previous studies, our Taylor initial values significantly improved the finite sample performances. We will then apply this method to simulation and empirical studies.

Results for Non-cointegrated x_t

Table 2 presents the simulation results for non-cointegrated x_t using $f_1(u_{t-1}, \gamma_1)$ and $f_2(u_{t-1}, \gamma_2)$. We can see from the table that both the NLSand CLS estimators converge when the sample size increases. And the CLS estimators perform better than the NLS estimators. For example, when $T = 1000$, the bias and standard deviation of CLS estimator in β_1 in $f_1(u_{t-1}, \gamma_1)$ is -0.00007 and 0.01574 respectively, but the values for the NLS estimator is 0.00835 and 0.01148.

The covariance of θ , β and γ are also smaller when the constraint is applied. Take the covariance of θ using $f_2(u_{t-1}, \gamma_2)$ as an example, $\text{cov}(\hat{\theta})$ dropped from 0.70877 and

Table 1: Simulation Results for Polynomial $f(u_{t-1}, \gamma)$ Using Different Initial Values

		θ_1	θ_2	β_1	β_2	γ_{11}	γ_{12}	γ_{13}
Initial Values = Taylor Initials								
T=100	Bias	0.00088	0.00026	-0.00079	0.00029	0.00326	-0.00064	0.00121
	std	0.00139	0.00105	0.00504	0.00504	0.00914	0.00451	0.00141
		0.00244		0.00461		0.01029		
T=500	Bias	-0.00013	-0.00008	-0.00040	-0.00058	0.00063	-0.00032	0.00146
	std	0.00041	0.00031	0.00068	0.00206	0.00436	0.00175	0.00043
		0.00167		0.00167		0.00472		
T=1000	Bias	-0.00005	-0.00003	-0.00025	-0.00012	0.00035	-0.00021	0.00087
	std	0.00026	0.00019	0.00043	0.00136	0.00319	0.00110	0.00026
		0.00045		0.00110		0.00339		
Initial Values = 0								
T=100	Bias	0.12214	0.35638	0.09401	-0.27546	2.40099	0.19899	-0.10567
	std	0.28186	0.45009	0.31824	1.10049	2.95226	0.67484	0.36090
		0.51793		1.02441		0.17287		
T=500	Bias	0.13182	0.47163	0.19141	-0.33712	2.25798	0.19733	-0.18554
	std	0.28545	0.52487	0.38507	1.13323	2.50154	0.78597	0.38406
		0.39734		0.57196		0.12342		
T=1000	Bias	0.15770	0.47870	0.21117	-0.25275	2.34776	0.30953	-0.20737
	std	0.26417	0.50324	0.04013	0.324009	0.21639	0.09167	0.06618
		0.15924		0.10229		0.07233		
Initial Values = True Values								
T=100	Bias	0.00008	0.00007	-0.00170	0.00082	0.00368	-0.00028	0.00080
	std	0.00127	0.00095	0.00196	0.00572	0.00735	0.00350	0.00174
		0.00222		0.00261		0.00832		
T=500	Bias	0.00003	0.00002	-0.00098	0.00085	0.00233	-0.00003	0.00068
	std	0.00029	0.00022	0.00069	0.00192	0.00330	0.00135	0.00060
		0.00050		0.00098		0.00362		
T=1000	Bias	0.00000	0.00001	-0.00091	0.00084	0.00023	-0.00003	0.00068
	std	0.00019	0.00014	0.00046	0.00133	0.00226	0.00090	0.00041
		0.00033		0.00065		0.00247		

0.06903, to 0.00536 and 0.00283 when $T = 500$ and $T = 1000$.

Table 2: Simulation Results for Non-cointegrated x_t Using f_1 and f_2

		NLS					Constrained-NLS				
		$f_1(u_{t-1}, \gamma_1)$									
		θ_1	θ_2	β_1	β_2	γ_1	θ_1	θ_2	β_1	β_2	γ_1
T = 100	Bias	0.38379	0.18386	0.08270	0.48694	-0.24803	-0.00145	-0.00116	-0.00038	0.00089	0.04358
	std	0.50727	0.32935	0.13342	0.04772	0.46857	0.01523	0.01683	0.00122	0.01254	0.08301
		0.63646			0.47723		0.02050		0.01191		
T = 500	Bias	0.38567	0.19677	0.07986	0.49866	-0.23763	-0.00408	-0.00063	-0.00012	0.00147	0.00911
	std	0.47487	0.30993	0.11830	0.01579	0.26452	0.00369	0.00432	0.00021	0.00364	0.03815
		0.60420			0.26785		0.00574		0.00345		
T = 1000	Bias	0.03802	0.01811	0.00835	0.04999	-0.01991	-0.00147	-0.00026	-0.00007	0.00100	0.00286
	std	0.04750	0.02966	0.01148	0.00124	0.02029	0.01892	0.01693	0.01574	0.02946	0.01798
		0.05939			0.02050		0.00249		0.00279		
		$f_1(u_{t-1}, \gamma_2)$									
		θ_1	θ_2	β_1	β_2	γ_2	θ_1	θ_2	β_1	β_2	γ_2
T = 100	Bias	0.44222	0.18241	0.08787	0.05589	0.47601	-0.00424	-0.00120	-0.00100	0.00334	0.04116
	std	0.57804	0.33512	0.12559	0.02178	0.58834	0.01781	0.01584	0.00222	0.01433	0.08129
		0.69034			0.58181		0.02291		0.01280		
T = 500	Bias	0.42377	0.16441	0.08132	0.05121	0.48900	-0.00147	-0.00052	-0.00036	0.00208	0.00771
	std	0.59056	0.32840	0.13094	0.00719	0.55783	0.00396	0.00411	0.00065	0.00553	0.03370
		0.70877			0.55450		0.00536		0.00493		
T = 1000	Bias	0.04422	0.01824	0.00559	0.04760	0.00879	-0.00074	-0.00032	-0.00017	0.00096	0.00287
	std	0.05780	0.03351	0.00218	0.05883	0.01256	0.00222	0.00174	0.00040	0.00367	0.01557
		0.06903			0.05818		0.00283		0.00328		

Table 3 presents the simulation results for non-cointegrated x_t using $f_3(u_{t-1}, \gamma_3, \gamma_4)$ and $f_4(u_{t-1}, \gamma_5, \gamma_6)$. When compared with the NLS estimators, CLS estimators have smaller magnitude for both bias and standard deviations. The biases of θ_1 in the case of CLS is -0.00177 while the value is 0.01467 in the case of NLS. And the CLS estimators also show a better convergence. As shown in the second panel, when sample size increases, the bias of β_2 decreases from 0.01092 to 0.00237.

Models with the two exponential functions (see table 4) also show similar performances. The NLS and CLS estimators converge when sample size increases and the CLS estimators perform better.

Table 5 present the results for model containing $f_7(u_{t-1}, \gamma_{11}, \gamma_{12}, \gamma_{13})$, we can also see

Table 3: Simulation Results for Non-cointegrated x_t Using f_3 and f_4

		NLS						Constrained-NLS					
		$f_3(u_{t-1}, \gamma_3, \gamma_4)$											
		θ_1	θ_2	β_1	β_2	γ_3	γ_4	θ_1	θ_2	β_1	β_2	γ_3	γ_4
T = 100	Bias	0.25080	0.11643	0.09701	0.09621	-0.02764	0.04677	-0.00512	-0.00957	0.00367	0.04089	0.00023	0.00084
	std	0.42010	0.27514	0.10589	0.14919	0.02840	0.04952	0.12251	0.09119	0.02431	0.11107	0.01023	0.02126
		0.49218		0.17846		0.02405		0.14820		0.11562		0.02353	
T = 500	Bias	0.18672	0.09059	0.07042	0.11776	-0.01412	0.02610	-0.00682	-0.00430	0.00062	-0.00060	-0.00083	0.00078
	std	0.37435	0.24955	0.09681	0.14953	0.01354	0.02486	0.02586	0.02294	0.00615	0.02334	0.00276	0.00475
		0.44802		0.17453		0.01163		0.03783		0.02383		0.00561	
T = 1000	Bias	0.01467	0.08110	0.05778	0.11680	-0.00923	0.01717	-0.00177	-0.00162	0.00013	-0.00149	-0.00033	0.00038
	std	0.03410	0.23593	0.09100	0.14950	0.00941	0.01754	0.01433	0.01388	0.00406	0.01529	0.00166	0.00248
		0.41141		0.17074		0.00825		0.02241		0.01568		0.00268	
		$f_4(u_{t-1}, \gamma_5, \gamma_6)$											
		θ_1	θ_2	β_1	β_2	γ_5	γ_6	θ_1	θ_2	β_1	β_2	γ_5	γ_6
T = 100	Bias	0.26070	0.13566	0.09572	0.10944	-0.00129	0.00539	-0.00839	-0.00700	0.00085	0.01092	-0.02653	0.04272
	std	0.41629	0.28334	0.10132	0.14225	0.00287	0.01948	0.05009	0.04422	0.01350	0.05372	0.02733	0.04743
		0.47705		0.17498		0.01708		0.06498		0.05641		0.02541	
T = 500	Bias	0.18304	0.09114	0.07063	0.12854	-0.00039	0.00245	-0.00153	-0.00013	-0.00044	0.00449	-0.01240	0.02233
	std	0.37174	0.24185	0.09417	0.14590	0.00071	0.00598	0.01367	0.01400	0.00352	0.01763	0.01216	0.02216
		0.43332		0.17804		0.00530		0.02039		0.01847		0.01036	
T = 1000	Bias	0.01397	0.06411	0.05101	0.12171	-0.00023	0.00163	-0.00015	0.00049	-0.00025	0.00237	-0.00777	0.01432
	std	0.03386	0.21123	0.08496	0.14666	0.00042	0.00383	0.00646	0.00684	0.00163	0.01559	0.00806	0.01490
		0.40072		0.17760		0.00342		0.01009		0.01588		0.00699	

a good convergence and an improvement in finite sample performance when constraint and truncation have been applied.

To conclude, for the non-cointegrated x_t , the proposed CLS estimators show a good convergence and a better performance than the normal NLS estimators. In the next section, we will investigate the performance of the estimators when x_t is cointegrated.

Table 4: Simulation Results for Non-cointegrated x_t Using f_5 and f_6

		NLS						Constrained-NLS					
		$f_5(u_{t-1}, \gamma_7, \gamma_8)$											
		θ_1	θ_2	β_1	β_2	γ_7	γ_8	θ_1	θ_2	β_1	β_2	γ_7	γ_8
T = 100	Bias	0.12540	0.08285	0.03502	0.10013	-0.00125	0.00465	-0.01512	-0.00850	0.00298	0.03600	0.00035	0.00010
	std	0.32644	0.22965	0.07947	0.14053	0.00291	0.01768	0.08939	0.09761	0.01671	0.10739	0.01028	0.02041
		0.41166		0.16238		0.01553		0.13624		0.10882		0.02240	
T = 500	Bias	0.07635	0.03312	0.02314	0.07846	-0.00040	0.00256	-0.00626	-0.00533	0.00098	0.00020	-0.00079	0.00069
	std	0.26124	0.15768	0.06617	0.13341	0.00061	0.00513	0.02448	0.02367	0.00617	0.02938	0.00270	0.00418
		0.33234		0.15343		0.00456		0.03878		0.02994		0.00500	
T = 1000	Bias	0.04853	0.02568	0.01525	0.06429	-0.00021	0.00148	-0.00145	-0.00138	0.00006	-0.00154	-0.00033	0.00027
	std	0.21269	0.13821	0.05665	0.12720	0.00038	0.00335	0.01348	0.01318	0.00342	0.01526	0.00176	0.00231
		0.27633		0.13912		0.00298		0.02050		0.01566		0.00267	
		$f_6(u_{t-1}, \gamma_9, \gamma_{10})$											
		θ_1	θ_2	β_1	β_2	γ_9	γ_{10}	θ_1	θ_2	β_1	β_2	γ_9	γ_{10}
T = 100	Bias	0.16972	0.09560	0.03762	0.09567	-0.00140	0.00279	-0.00253	-0.00113	0.05286	0.11522	-0.00797	0.02183
	std	0.36696	0.24840	0.08178	0.13985	0.00590	0.02946	0.02819	0.02091	0.17887	0.31808	0.00821	0.05086
		0.45088		0.15968		0.02947		0.04905		0.36180		0.04597	
T = 500	Bias	0.13362	0.08659	0.03314	0.08628	-0.00043	0.00218	-0.00254	-0.00179	0.01126	0.01520	-0.00432	0.02071
	std	0.33483	0.23097	0.07623	0.13596	0.00139	0.01472	0.01036	0.00771	0.02667	0.13611	0.00234	0.02118
		0.42320		0.15627		0.01379		0.01806		0.13714		0.01923	
T = 1000	Bias	0.08091	0.04687	0.02416	0.08304	-0.00009	0.00082	-0.00177	-0.00128	0.00945	-0.00417	-0.00394	0.02014
	std	0.26874	0.18120	0.06819	0.13751	0.00020	0.00334	0.00698	0.00520	0.01713	0.08853	0.00161	0.01523
		0.34376		0.15229		0.00317		0.01218		0.08865		0.01382	

Simulation Results for Cointegrated x_t

Table 6 to 9 present the simulation results on co-integrated x_t using Taylor initial values. Table 6 shows the results for model containing nonlinear component $f_1(u_{t-1}, \gamma_1) = \sin(u_t + \gamma_1)$ and $f_2(u_{t-1}, \gamma_2) = \cos(u_t + \gamma_2)$. From the table we can see that the constrained CLS estimators perform better than the NLS estimators. Bias, standard deviation and covariance of the estimators are lower in the constrained least square case than in the nonlinear least square case. For example, for model containing f_1 , the absolute value

Table 5: Simulation Results for Non-cointegrated x_t Using f_7

		NLS							Constrained-NLS						
		θ_1	θ_2	β_1	β_1	γ_{11}	γ_{12}	γ_{13}	θ_1	θ_2	β_1	β_1	γ_{11}	γ_{12}	γ_{13}
T = 100	Bias	0.02111	-0.01598	30.87179	-0.95731	-0.01892	-0.60074	0.72155	0.00286	0.00084	0.06327	-0.00989	0.00370	-0.01088	0.00725
	std	0.36946	0.31152	0.74012	0.74312	0.29472	0.17836	0.14145	0.03604	0.02714	0.36089	0.05816	0.02418	0.03986	0.11360
		0.48890		0.74443			0.14232		0.05138		0.36636			0.11006	
T = 500	Bias	0.02983	0.02140	3.07132	-0.65861	0.01327	-0.05536	0.16146	0.00066	0.00026	0.02231	-0.00085	0.00025	-0.00126	0.00019
	std	0.47050	0.43007	0.19241	0.285891	0.41959	0.47356	0.33892	0.00355	0.00347	0.11853	0.02182	0.00301	0.00422	0.02105
		0.07039		0.19932			0.03417		0.00581		0.12056			0.02087	
T = 1000	Bias	0.00261	-0.00316	2.48519	-0.17601	0.00291	-0.01104	-0.01521	0.00014	0.00019	0.00743	-0.00007	0.00014	-0.00050	-0.00008
	std	0.20383	0.17837	0.1113794	0.19016	0.20954	0.16493	0.19888	0.00155	0.00138	0.10818	0.01050	0.00141	0.00219	0.00929
		0.00300		0.11301			0.01985		0.00263		0.10870			0.00876	

of bias of θ_1 is 0.00818 when using NLS and 0.00129 when using CLS estimator (sample size $T = 1000$).

The estimators also show a good convergence. Take the covariance of γ in the second panel as an example, the covariance of γ decrease from 0.01916 to 0.00242 when sample size T rises from 100 to 1000.

Similarly for $f_3(u_{t-1}, \gamma_3, \gamma_4) = \sin(\gamma_3 u_t + \gamma_4)$ and $f_4(\gamma_5 u_{t-1}, \gamma_6) = \cos(\gamma_5 u_t + \gamma_6)$, both NLS and CLS estimators converge and the CLS estimators perform better. For example, in the first panel of table 7, the absolute value of bias of θ_1 using $f_3(u_{t-1}, \gamma_3, \gamma_4)$ drops from 0.00219 to 0.00062 in the case of CLS and decreases from 0.01336 to 0.00201 in the case of NLS.

And in most cases, the CLS estimators have smaller bias, standard deviation and covariance. As shown in the second panel of table 7, the covariance of CLS estimator γ ($\text{cov}(\hat{\gamma})$) is smaller when $T = 1000$ (0.05015 for CLS, and 0.09848 for NLS), even though when sample size $T = 500$, it is slightly higher (0.19193 for CLS and 0.17287 for NLS).

For the models containing two exponential functions $f_5(u_{t-1}, \gamma_7, \gamma_8) = 1 - e^{-\gamma_7(u_{t-1} - \gamma_8)^2}$ and $f_6(u_{t-1}, \gamma_9, \gamma_{10}) = \gamma_9 e^{-\gamma_{10} u_{t-1}^2}$, we can see that the NLS estimators does not have good convergence, but after applying constraint, the convergence has significantly improved. For example, in the case of CLS, the biases of β_1 is 0.00060 and 0.00051 when $T = 100$ and 1000 respectively, and the corresponding values in the case of NLS are 0.08371 and 0.00105.

The CLS estimators also have smaller biases, standard deviations and covariances. Take β in $f_6(u_{t-1}, \gamma_9, \gamma_{10})$ as an example, the covariance of the CLS estimator is 0.00263

Table 6: Simulation Results for Cointegrated x_t Using Models with f_1 and f_2

		NLS					Constrained-NLS				
		$f_1(u_{t-1}, \gamma_1)$									
		θ_1	θ_2	β_1	β_2	γ_1	θ_1	θ_2	β_1	β_2	γ_1
T = 100	Bias	0.00221	0.01180	-0.01443	0.01320	0.00447	0.01287	0.01004	-0.01604	-0.00325	-0.02298
	std	0.09413	0.08928	0.05052	0.06048	0.52541	0.01474	0.01180	0.04778	0.05835	0.46140
		0.08751		0.03648			0.02653		0.04417		
T = 500	Bias	-0.00776	0.01514	-0.01165	0.01131	-0.00464	0.00247	0.00186	-0.01223	0.00879	-0.01146
	std	0.05713	0.04579	0.02192	0.02447	0.30383	0.00289	0.00219	0.02094	0.02295	0.29016
		0.04800		0.01013			0.00508		0.00918		
T = 1000	Bias	-0.00818	0.01622	-0.01119	0.01126	-0.00584	0.00129	0.00097	-0.01176	0.01021	-0.02066
	std	0.06111	0.04695	0.01541	0.01690	0.29261	0.00149	0.00112	0.01526	0.01632	0.27447
		0.05325		0.00590			0.00262		0.00471		
		$f_2(u_{t-1}, \gamma_2)$									
		θ_1	θ_2	β_1	β_2	γ_1	θ_1	θ_2	β_1	β_2	γ_2
T = 100	Bias	0.00069	0.00276	-0.00646	0.00180	0.03309	-0.00189	-0.00192	0.00104	-0.00143	0.04245
	std	0.04767	0.03619	0.03458	0.04583	0.12469	0.02647	0.02972	0.01103	0.01648	0.08817
		0.08369		0.04306			0.03984		0.01916		
T = 500	Bias	0.00068	0.00075	-0.01248	0.01028	-0.00206	-0.00010	-0.00026	-0.00049	0.00061	0.00770
	std	0.01564	0.01175	0.01493	0.02015	0.05825	0.00622	0.00698	0.00272	0.00421	0.04282
		0.02738		0.01652			0.00927		0.00518		
T = 1000	Bias	-0.00012	0.00005	-0.01275	0.01034	0.00029	-0.00015	0.00087	-0.00041	0.00051	0.00100
	std	0.01206	0.00905	0.01188	0.01482	0.04136	0.00329	0.00330	0.00156	0.00191	0.02102
		0.02110		0.01129			0.00476		0.00242		

Table 7: Simulation Results for Cointegrated x_t Using Models with f_3 and f_4

		NLS						Constrained-NLS					
		$f_3(u_{t-1}, \gamma_3, \gamma_4)$											
		θ_1	θ_2	β_1	β_2	γ_3	γ_4	θ_1	θ_2	β_1	β_2	γ_3	γ_4
T = 100	Bias	-0.01336	-0.00146	0.00040	0.00012	0.00258	0.03875	-0.00219	0.00367	-0.01027	0.00355	0.00143	-0.00586
	std	0.09908	0.10823	0.01118	0.01976	0.02365	0.11074	0.07270	0.05655	0.03583	0.05240	0.06347	0.12251
		0.14788		0.02250		0.11450		0.12888		0.05136		0.13895	
T = 500	Bias	-0.00561	-0.00664	-0.00106	0.00100	0.00074	0.00084	0.00039	0.00178	-0.01354	0.00635	-0.00269	-0.00414
	std	0.02504	0.02534	0.00283	0.00462	0.00631	0.03351	0.03891	0.02937	0.01772	0.02257	0.02483	0.04649
		0.03833		0.00539		0.03384		0.06821		0.02083		0.05447	
T = 1000	Bias	-0.00201	-0.00204	-0.00048	0.00044	0.00039	-0.00138	0.00062	0.00143	-0.01299	0.00738	-0.00171	-0.00021
	std	0.01434	0.01451	0.00197	0.00230	0.00392	0.01576	0.03144	0.02371	0.01291	0.01631	0.01754	0.03414
		0.02283		0.00277		0.01611		0.05511		0.01493		0.04048	
		$f_4(u_{t-1}, \gamma_5, \gamma_6)$											
		θ_1	θ_2	β_1	β_2	γ_5	γ_6	θ_1	θ_2	β_1	β_2	γ_5	γ_6
T = 100	Bias	-0.00462	0.00898	-0.00485	0.00572	0.00210	0.03106	-0.00283	0.00192	0.00022	-0.00015	-0.01107	-0.00375
	std	0.10139	0.10403	0.03259	0.05225	0.01558	0.10063	0.06346	0.04934	0.01071	0.02085	0.05994	0.18408
		0.14118		0.04906		0.17287		0.11249		0.02418		0.19193	
T = 500	Bias	-0.00586	0.00356	-0.01139	0.01223	0.00094	0.00065	-0.01064	-0.00614	-0.00082	0.00065	-0.00232	-0.02078
	std	0.01965	0.02729	0.01540	0.02242	0.00549	0.03119	0.04250	0.03141	0.00315	0.00483	0.02115	0.07684
		0.03187		0.02015		0.12557		0.07384		0.00576		0.07694	
T = 1000	Bias	-0.00286	0.00068	-0.00984	0.01005	0.00026	-0.00096	-0.00967	-0.00599	-0.00052	0.00048	-0.00040	-0.01090
	std	0.01282	0.01323	0.01171	0.01616	0.00364	0.01763	0.03508	0.02570	0.00194	0.00233	0.01420	0.05158
		0.01564		0.01282		0.09848		0.06074		0.00272		0.05015	

and that of the NLS estimator is 0.01184.

Table 8: Simulation Results for Cointegrated x_t Using Models with f_5 and f_6

		NLS						Constrained-NLS					
		$f_5(u_{t-1}, \gamma_7, \gamma_8)$											
		θ_1	θ_2	β_1	β_2	γ_7	γ_8	θ_1	θ_2	β_1	β_2	γ_7	γ_8
T = 100	Bias	0.14852	0.07716	-0.00060	-0.00069	0.03979	0.09704	0.00049	0.00707	-0.08371	0.00270	0.05869	0.11357
	std	0.36721	0.25730	0.00983	0.01876	0.08946	0.14248	0.08064	0.06468	0.03280	0.04974	0.22359	0.36681
		0.47514		0.02122		0.16524		0.14459		0.04685		0.44678	
T = 500	Bias	0.06033	0.02538	-0.00080	0.00085	0.03530	0.09690	-0.00189	0.00011	-0.01111	0.00823	0.00059	0.02411
	std	0.25251	0.16061	0.00290	0.00427	0.08116	0.14316	0.03955	0.02972	0.01524	0.01987	0.04029	0.17323
		0.30811		0.00490		0.16249		0.06920		0.01641		0.17454	
T = 1000	Bias	0.04737	0.02568	-0.00051	0.00050	0.02912	0.08033	-0.00377	-0.00197	-0.00105	0.00843	0.00041	-0.00583
	std	0.21925	0.14210	0.00204	0.00215	0.07485	0.13657	0.02952	0.02203	0.01198	0.01481	0.02361	0.11419
		0.28125		0.00249		0.15389		0.05151		0.01177		0.11498	
		$f_6(u_{t-1}, \gamma_9, \gamma_{10})$											
		θ_1	θ_2	β_1	β_2	γ_9	γ_{10}	θ_1	θ_2	β_1	β_2	γ_9	γ_{10}
T = 100	Bias	0.29939	0.12435	-0.00836	0.00577	0.09685	0.86918	0.00239	0.00565	-0.00015	0.00038	0.10008	0.10486
	std	0.44703	0.31855	0.03431	0.04555	0.26677	1.16532	0.06176	0.04835	0.01144	0.01696	0.10519	0.14436
		0.52722		0.04150		1.23387		0.10976		0.01892		0.16633	
T = 500	Bias	0.20686	0.12096	-0.01268	0.01065	0.01278	0.33971	-0.00633	-0.00314	-0.00108	0.00100	0.08506	0.11410
	std	0.39309	0.27335	0.01578	0.02035	0.09200	0.81052	0.04018	0.03030	0.00304	0.00424	0.09984	0.14511
		0.47572		0.01677		0.82640		0.07041		0.00456		0.16128	
T = 1000	Bias	0.18891	0.09882	-0.01164	0.01017	0.00430	0.17839	-0.00107	-0.00681	-0.00047	0.00036	0.07620	0.11676
	std	0.37535	0.25110	0.01210	0.01538	0.06249	0.54192	0.03382	0.02468	0.00180	0.00239	0.09744	0.14438
		0.45836		0.01184		0.56098		0.05847		0.00263		0.16354	

Table 9 presents the simulation results for the model containing polynomial function $f_7(u_{t-1}, \gamma_{11}, \gamma_{12}, \gamma_{13}) = \gamma_{11} + \gamma_{12}u_{t-1} + \gamma_{13}u_{t-1}^2$. Both NLS and CLS estimators have good convergence and the CLS shows a better performance for β and γ .

As for the convergence, take β_1 as an example, the absolute value of bias for the NLS estimator $\hat{\beta}$ decreases from 0.00056 to 0.00001 as sample size T increases from 100 to 1000. At the same time, the absolute value of bias for the CLS estimator $\bar{\beta}$ decreases from 0.00079 to 0.00025.

The constraint and truncation conditions we applied improve the finite sample performance for all the estimators, and the effect is more significant for the estimator γ . For example, when T = 1000, the covariance of β in the case of NLS is 0.00190 and the value is 0.00110 in the case of CLS. And for the covariance of γ , the value in the case of CLS is 0.00339, which is much lower than 0.01231 in the case of NLS.

From the simulation results above, we can conclude that:

Table 9: Simulation Results for Cointegrated x_t Using Models with f_7

		NLS							Constrained-NLS						
		θ_1	θ_2	β_1	β_1	γ_{11}	γ_{12}	γ_{13}	θ_1	θ_2	β_1	β_1	γ_{11}	γ_{12}	γ_{13}
T = 100	Bias	0.00018	-0.00018	-0.00056	0.00037	0.02711	-0.00147	0.00020	0.00088	0.00026	-0.00079	0.00029	0.00326	-0.00064	0.00121
	std	0.00407	0.00335	0.00171	0.01482	0.07001	0.00886	0.00308	0.00139	0.00105	0.00161	0.00504	0.00914	0.00451	0.00141
		0.00528		0.01502			0.07063		0.00244		0.00461			0.01029	
T = 500	Bias	0.00006	0.00003	-0.00003	0.00024	0.00261	-0.00072	0.00026	-0.00013	-0.00008	-0.00040	-0.00058	0.00063	-0.00032	0.00146
	std	0.00051	0.00040	0.00039	0.00354	0.01664	0.00315	0.00047	0.00041	0.00031	0.00068	0.00206	0.00436	0.00175	0.00043
		0.00068		0.00357			0.01695		0.00071		0.00167			0.00472	
T = 1000	Bias	0.00008	0.00004	-0.00001	-0.00014	0.00218	-0.00008	-0.00006	-0.00005	-0.00003	-0.00025	-0.00012	0.00035	-0.00021	0.00087
	std	0.00026	0.00015	0.00015	0.00194	0.01219	0.00173	0.00020	0.00026	0.00019	0.00043	0.00136	0.00319	0.00110	0.00026
		0.00032		0.00190			0.01231		0.00045		0.00110			0.00339	

1. The Taylor initial values can help improve the finite sample performances of the estimators.
2. Both the NLS and CLS estimators converge when sample size increases. But the constrained least square method tend to give better convergence in most cases.
3. The CLS consistently perform better than the normal NLS for most functional forms. This implies that the constraint and truncation condition we proposed in section 2 do help improve the finite sample performances.
4. Among models with the 7 different functional forms, the one with polynomial functional form tend to provide the best results, but models with the two exponential functions do not perform as well as other ones.

As shown in table 9, the standard deviation of θ using CLS is 0.00045 when T=1000, which is much lower than this value in other functional cases(for example, the corresponding value is 0.00262 in $f_1(u_{t-1}, \gamma_0)$ and 0.00476 in $f_2(u_{t-1}, \gamma_0)$).

5. Models using cointegrated x_t have a better finite sample performance than using the non-cointegrated x_t . As presented in table 10, the bias of θ using cointegrated x_t is at least one magnitude smaller than using the non-cointegrated x_t .

Therefore, in the empirical study, we will focus on the constrained least square method as the CLS estimators consistently provide better performances. In terms of predictors and model estimation, we will consider cointegrated predictors and use Taylor initial values to start the iterative estimation procedure.

Table 10: Simulation Results for Cointegrated x_t and Non-cointegrated x_t Using f_7

		Cointegrated x_t							Non-cointegrated x_t						
		θ_1	θ_2	β_1	β_2	γ_1	γ_2	γ_3	θ_1	θ_2	β_1	β_2	γ_1	γ_2	γ_3
T = 100	Bias	0.00088	0.00026	-0.00079	0.00029	0.00326	-0.00064	0.00121	0.00286	0.00084	0.06327	-0.00989	0.00370	-0.01088	0.00725
	std	0.00139	0.00105	0.00161	0.00504	0.00914	0.00451	0.00141	0.03604	0.02714	0.36089	0.05816	0.02418	0.03986	0.11360
		0.00244		0.00461			0.01029		0.05138		0.36636			0.11006	
T = 500	Bias	-0.00013	-0.00008	-0.0004	-0.00058	0.00063	-0.00032	0.00146	0.00066	0.00026	0.02231	-0.00085	0.00025	-0.00126	0.00019
	std	0.00041	0.00031	0.00068	0.00206	0.00436	0.00175	0.00043	0.00355	0.00347	0.11853	0.02182	0.00301	0.00422	0.02105
		0.00071		0.00167			0.00472		0.00581		0.12056			0.02087	
T = 1000	Bias	-0.00005	-0.00003	-0.00025	-0.00012	0.00035	-0.00021	0.00087	0.00014	0.00019	0.00743	-0.00007	0.00014	-0.00050	-0.00008
	std	0.00026	0.00043	0.00043	0.00136	0.00319	0.0011	0.00026	0.00155	0.00138	0.10818	0.01050	0.00141	0.00219	0.00929
		0.00045		0.0011			0.00339		0.00263		0.10870			0.00876	

4 Empirical Study

We have examined the finite sample properties in the previous section using Monte Carlo simulation study. To illustrate the use of our partially nonlinear model in the real world, we conduct the in-sample and out-of-sample prediction exercises using U.S. stock market returns data. The datasets is available from Amit Goyal's website and it is quarterly data ranging from 1956 Q1 to 2018 Q4 .

The dependent variable, stock return, is measured as continuously compound returns on the S&P 500 index. Predictors used in [Welch and Goyal \(2008\)](#) include dividend-price ratio (log), dividend yield (log), earnings-price ratio (log), dividend-payout ratio (log), and other 11 predictors.

In our study, we want to evaluate the performance of the partially nonlinear models when the non-stationary predictors are co-integrated, therefore we choose the following 4 variable pairs from the [Welch and Goyal \(2008\)](#) datasets (as in [Zhou et al. \(2018\)](#)) and another set of variable from [Lettau and Ludvigson \(2001\)](#), which have all been found to be co-integrated :

- co1: dividend-price ratio (dp) and dividend yield (dy).

Dividend-price ratio is the difference between the log of dividends and the log of stock prices; dividend yield is the difference between the log of dividends and the log of lagged stock prices.

- co2: T-bill rate (tbl) and long-term yield (lty).

T-bill rate is the interest rate on a three-month Treasury bill; long-term yield stands for the long-term government bond yield.

- co3: dividend-price ratio and earning-price ratio.

The earning-price ratio is the difference between the log of earnings on the S&P 500 index and the log of stock prices.

- co4: baa- and aaa-rated corporate bonds yields.

Figure 4 plots the time series of the co-integrated variable pairs. It is clear that the variables in each plot are not stationary and have similar shape. Especially for the first pair, "co1", the d/p ratio and the dividend yield are very close to each other.

Figure 4: Time Series Plots of Co-integrated Variables

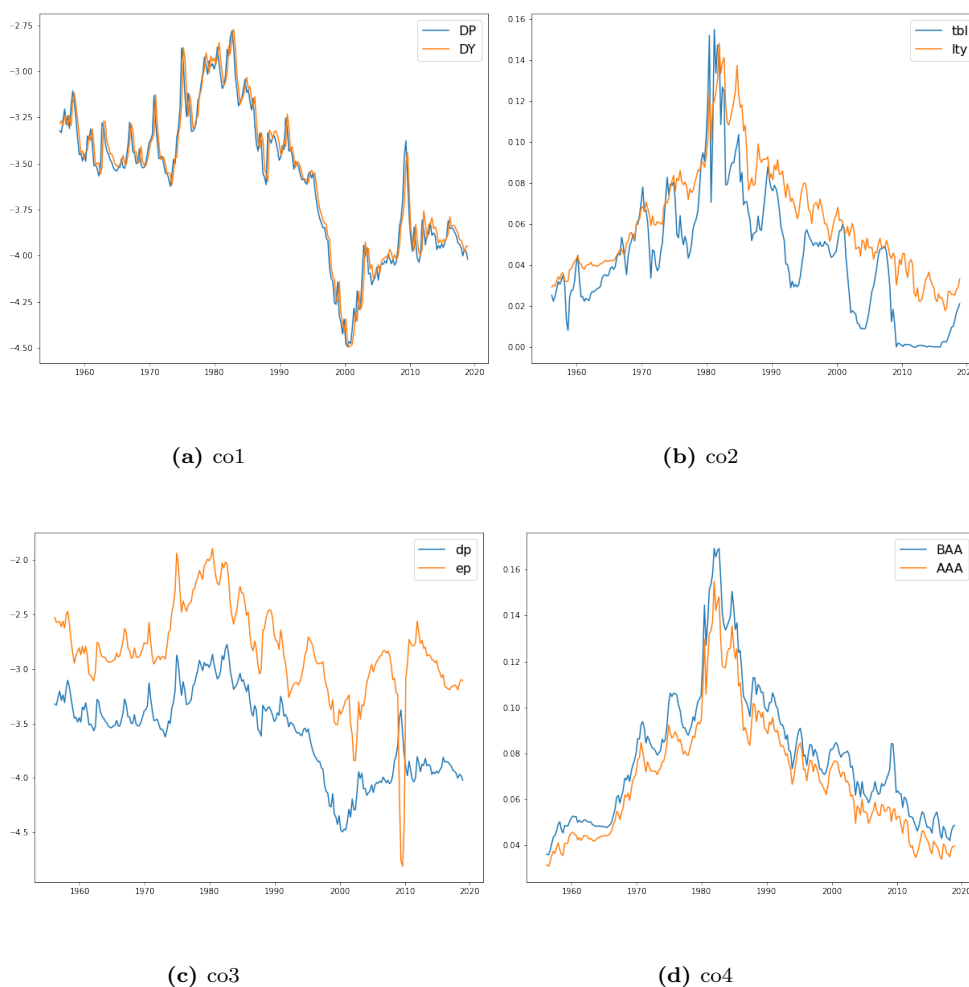
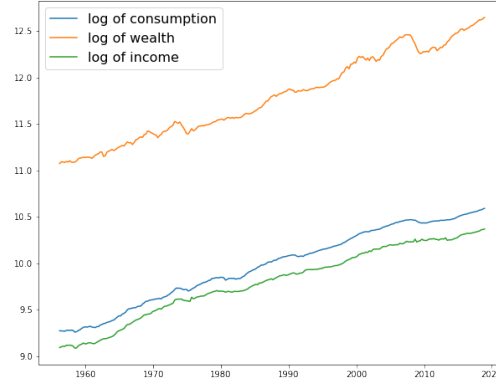


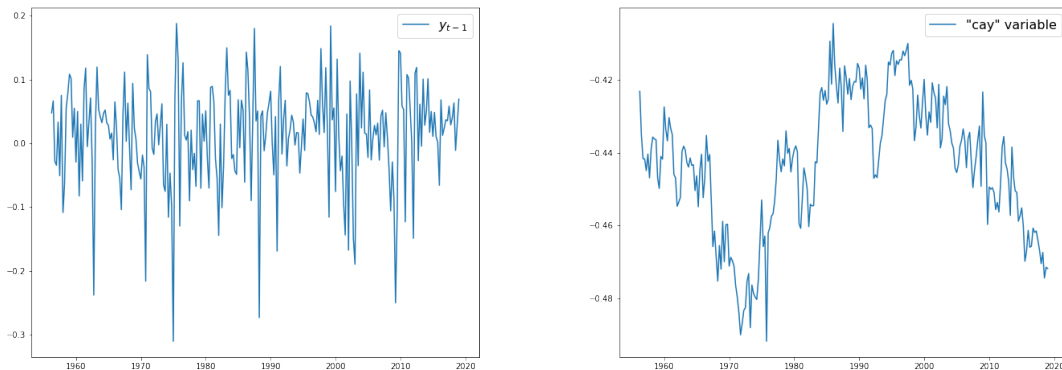
Figure 5 shows the three variables used in Lettau and Ludvigson (2001). It is clear that log consumption, log asset wealth and log labor income share a common stochastic trend.

Figure 5: "cay" variable



Apart from the non-stationary variables, the partially nonlinear models also include stationary predictors: the lagged stock return (y_{t-1}) and the regression residual (the "cay" variable, hereafter) from the study of Lettau and Ludvigson (2001). In their study, they show that the three variables are cointegrated and share a common trend. The deviations from this shared trend is stationary and can be used as a predictor for stock return. Figure 6 below presents the two variables.

Figure 6: Time Series Plots of Stationary Variables



(a) lag of dependent variable

(b) "cay" variable

Therefore in the partially nonlinear models we consider:

$$y_t = \beta_1 y_{t-1} + \beta_2 w_{t-1} + f(x'_{t-1} \theta, \gamma) + e_t, \quad e_t \sim i.i.d.N(0, 1), \quad t = 2, \dots, T,$$

where the dependent variable, y_t , is the equity premium defined as the S&P500 value-weighted log excess returns. y_{t-1} is the lagged equity premium, x_{t-1} are the co-integrated variables from [Zhou et al. \(2018\)](#), and w_{t-1} is the regression residual, the "cay" variable, from the [Lettau and Ludvigson \(2001\)](#).

In terms of the nonlinear part $f(x'_{t-1} \theta, \gamma)$, we consider the following 7 nonlinear functions that have been discussed in the simulation before. It includes trigonometric functions, exponential functions and polynomial functions. And these partially nonlinear models in the empirical study can be written as:

$$\begin{aligned} \sin : g_1(u_{t-1}, \gamma_1) &= \beta z'_{t-1} + \sin(u_{t-1} + \gamma_1), \\ \cos : g_2(u_{t-1}, \gamma_2) &= \beta z'_{t-1} + \cos(u_{t-1} + \gamma_2), \\ \text{scale_sin} : g_3(u_{t-1}, \gamma_3, \gamma_4) &= \beta z'_{t-1} + \sin(\gamma_3 u_{t-1} + \gamma_4), \\ \text{scale_cos} : g_4(u_{t-1}, \gamma_5, \gamma_6) &= \beta z'_{t-1} + \cos(\gamma_5 u_{t-1} + \gamma_6), \\ \text{exp_shift} : g_5(u_{t-1}, \gamma_7, \gamma_8) &= \beta z'_{t-1} + 1 - e^{-\gamma_7(u_{t-1} - \gamma_8)^2} \\ \text{exp} : g_6(u_{t-1}, \gamma_9, \gamma_{10}) &= \beta z'_{t-1} + \gamma_9 e^{-\gamma_{10} u_{t-1}^2} \\ \text{Polynomial} : g_7(\hat{u}_{t-1}, \gamma_{11}, \gamma_{12}, \gamma_{13}) &= \beta z'_{t-1} + \gamma_{11} + \gamma_{12} u_{t-1} + \gamma_{13} u_{t-1}^2 \end{aligned}$$

where $\beta = (\beta_1, \beta_2)$, $z'_{t-1} = (y_{t-1}, w_{t-1})$, and $u_{t-1} = x'_{t-1} \theta$.

In addition, we also include a linear functional form with single-index:

$$\text{constrained_linear} : g_8(u_{t-1}, \gamma_{14}, \gamma_{15}) = \gamma_{14} + \beta z'_{t-1} + \gamma_{15}(x_{1,t-1} \theta_1 + x_{2,t-1} \theta_2).$$

This model is a special case of the polynomial function g_7 where $\gamma_{13} = 0$.

For all the 8 functional forms, we set $\theta_1^2 + \theta_2^2 = 1$ and will adopt the constrained nonlinear least square method described in section 2 to estimate. And as mentioned before, when minimizing the nonlinear least squares:

$$S_T(\beta, \theta, \gamma) = \sum_{t=1}^T (y_t - g(u_{t-1}, \gamma))^2$$

The gradient equation:

$$\frac{\partial S_T(\alpha)}{\partial \alpha}$$

does not have a closed solution, so we need to use an iterative algorithm. Following our discussion in the previous section, we adopt the 2-step procedure to calculate the Taylor initial values. We estimate the linear regression to get $\hat{\eta}$:

$$x_1 = \eta x_2 + e_t, \quad e_t \sim i.i.d.N(0, 1), \quad t = 2, \dots, T$$

and obtain the initial values for θ : $\theta_0 = (\frac{1}{\sqrt{1 + \hat{\eta}^2}}, \frac{-\hat{\eta}}{\sqrt{1 + \hat{\eta}^2}})$.

Then we bring u_{t-1} back into $f(u_{t-1}, \gamma)$ and substitute the nonlinear function $f(u_{t-1}, \gamma)$ by its first or second order Taylor series expansion and estimate the following linear regression to obtain the initial values for β and γ .

$$\begin{aligned} \sin : \tilde{g}_1(\hat{u}_{t-1}, \gamma_1) &= (\gamma_1 + \hat{u}_{t-1}) + \beta z'_{t-1}, \\ \cos : \tilde{g}_2(\hat{u}_{t-1}, \gamma_2) &= 1 - (\gamma_2 + \hat{u}_{t-1})^2 + \beta z'_{t-1}, \\ \sin_scaled : \tilde{g}_3(\hat{u}_{t-1}, \gamma_3, \gamma_4) &= \gamma_4 + \gamma_3 \hat{u}_{t-1} + \beta z'_{t-1}, \\ \cos_scaled : \tilde{g}_4(\hat{u}_{t-1}, \gamma_5, \gamma_6) &= 1 - (\gamma_6 + \gamma_5 \hat{u}_{t-1})^2 + \beta z'_{t-1}, \\ \exp_shift : \tilde{g}_5(\hat{u}_{t-1}, \gamma_7, \gamma_8) &= \gamma_7 \hat{u}_{t-1}^2 - 2\gamma_8 \gamma_7 \hat{u}_{t-1} + \gamma_7 \gamma_8^2 + \beta z'_{t-1} \\ \exp : \tilde{g}_6(\hat{u}_{t-1}, \gamma_9, \gamma_{10}) &= \gamma_9(1 - \gamma_{10} \hat{u}_{t-1}^2 + \frac{\gamma_{10}^2 \hat{u}_{t-1}^4}{2}) + \beta z'_{t-1}, \\ \text{Polynomial} : \tilde{g}_7(\hat{u}_{t-1}, \gamma_{11}, \gamma_{12}, \gamma_{13}) &= \gamma_{11} + \gamma_{12} \hat{u}_{t-1} + \gamma_{13} \hat{u}_{t-1}^2 + \beta z'_{t-1}, \\ \text{constrained_linear} : \tilde{g}_8(\hat{u}_{t-1}, \gamma_{14}, \gamma_{15}) &= \gamma_{14} + \gamma_{15} \hat{u}_{t-1} + \beta z'_{t-1} \end{aligned}$$

where $\beta = (\beta_1, \beta_2)$, $z'_{t-1} = (y_{t-1}, w_{t-1})$.

In the simulation section, we have shown that by using Taylor-initials, the convergence of the estimators have improved significantly. In this section, we will investigate the empirical performances of our partially nonlinear models using these Taylor-initials.

4.1 In-sample Results

In this section, we use the complete sample from 1956 Q1 to 2018 Q4 to investigate the in-sample performances of our partially nonlinear models. The full sample results can be found in the appendix (table 14). In this section, we use in-sample R^2 (denoted by R_{IS}^2) to examine the in-sample performance of our models. The in-sample R_{IS}^2 is defined as:

$$R_{IS}^2 = 1 - \frac{\sum_{t=1}^n (y_t - \hat{y}_t)^2}{\sum_{t=1}^n (y_t - \bar{y})^2} \quad (4.1)$$

where y_t is the observed stock return in time t , \bar{y} is the predicted return from the benchmark model, and \hat{y}_t is the corresponding predicted stock return.

R_{IS}^2 can also be rewritten as:

$$R_{IS}^2 = 1 - \frac{MSE_{CLS}}{MSE_{bm}} \quad (4.2)$$

where MSE_{bm} is the mean squared error of benchmark model and $MSE_{CLS} = 1/n \sum_{t=1}^n (y_t - \hat{y}_t)^2$ is the mean squared error of our partially nonlinear models. In equation (4.2), if R_{IS}^2 for a given model is positive, it indicates that the model outperforms the benchmark model, and the bigger the value is, the better the corresponding model performs.

In the study of [Welch and Goyal \(2008\)](#), they found that sample mean is a competitive model in stock return prediction. Therefore, we use the sample mean model as one of our benchmark. We also consider some commonly used time series models and the nonlinear model we used in chapter 2 as benchmarks. The benchmark models we consider are as follows:

- Sample mean model:

$$y_t = \frac{1}{t-1} \sum_{i=1}^{t-1} y_i$$

- AR1:

$$y_t = \beta_1 y_{t-1} + \epsilon_t$$

- AR2:

$$y_t = \beta_1 y_{t-1} + \beta_2 y_{t-2} + \epsilon_t$$

- AR1 model with "cay" variable:

$$y_t = \beta_1 y_{t-1} + \beta_2 cay_{t-1} + \epsilon_t$$

- Nonlinear single-index model:

$$y_t = f(x'_{t-1} \theta, \beta) + \epsilon_t,$$

where $\epsilon_t \sim i.i.d.N(0, 1)$.

The results of R_{IS}^2 against sample mean model is reported in table 11. Among the 8 functional forms, g_3 , g_4 , g_5 , g_7 and g_8 provide positive R_{IS}^2 for all 4 variable combinations, which means the 5 functional forms have better in-sample performances than historical benchmark. And for g_1 , g_2 and g_6 , they can outperform sample mean model for some of the variable combinations.

Table 11: Results of R_{IS}^2 for all the models (benchmark: sample mean model)

variables	function	R_{IS}^2	function	R_{IS}^2	function	R_{IS}^2	function	R_{IS}^2
co1		-0.37483		0.00656		0.02287		0.01445
co2		0.01603		0.01633		0.00000		0.01626
co3	g_1	-5.82166	g_3	0.00115	g_5	0.02376	g_7	0.01814
co4		-0.00622		0.01026		0.00000		0.01493
co1		-0.57967		0.01183		-0.07239		0.00780
co2		-0.03409		0.01633		-0.02301		0.01633
co3	g_2	-5.50946	g_4	0.00618	g_6	0.01751	g_8	0.00077
co4		0.00615		0.01026		-0.02565		0.01025

Table 12 presents the the in-sample R_{IS}^2 against the nonlinear models we used in chapter 2. We can also see that our partially nonlinear models perform better for some variables and models. For example, for the variable combination co4 (baa and aaa rated bonds), models g_4 , g_6 , g_8 can provide a better in-sample performance. It indicates that after including stationary variables, we can improve the in-sample performance in some cases.

The in-sample R_{IS}^2 results against other benchmark models can be found in the appendix (put later).

4.2 OOS Results

OOS Performance Compared with Historical Average

Since the existing literatures show that the evidence for stock return predictability only hold for in-sample, in this section, we investigate how our models perform out-of-sample. Following Campbell and Thompson (2008), we use the OOS R^2 (denoted by R_{OOS}^2) to

Table 12: Results of R_{IS}^2 for all the models (benchmark: Nonlinear Model)

variables	function	R_{IS}^2	function	R_{IS}^2	function	R_{IS}^2	function	R_{IS}^2
co1		0.31283		-0.00717		-0.08370		0.02620
co2		-0.00712		0.00240		-0.01162		-0.02511
co3	g_1	0.78506	g_3	0.01185	g_5	-1.20501	g_7	-0.02166
co4		-0.01189		-0.00214		-0.81296		-0.40862
co1		0.31278		-0.00985		-0.13675		-0.01857
co2		-0.00711		0.00312		0.09928		0.00240
co3	g_2	0.78993	g_4	0.09388	g_6	-0.17578	g_8	-0.00073
co4		-0.02822		0.01147		0.09928		-0.00181

measure the forecasting performance. The R_{OOS}^2 is defined as:

$$R_{OOS,j,n,R}^2 = 1 - \frac{\sum_{r=1}^R (y_{n+r,j} - \hat{y}_{n+r,j})^2}{\sum_{r=1}^R (y_{n+r,j} - \bar{y}_{n+r,j})^2} \quad (4.3)$$

where n is the sample size of initial data to get a regression estimate at the start of evaluation period, R is the total number of expansive windows. In our case, $n = 128$ (from 1956 Q1 to 1987 Q4) and the maximum of R is 124 (from 1988 Q1 to 2018 Q4). We also set $j = 1$ because we only consider 1-step forecast. To make the notation simpler, we will ignore the subscript j in the rest of the chapter.

In the above definition, \hat{y}_{n+r} is the 1-step predicted return in the r -th window. \bar{y}_{n+r} is the sample mean of observations using the information up to $n + r - 1$, y_{n+r} is the observed return in period $n + r$.

To generate the first out-of-sample stock return forecast, we use the first $n-1$ pairs of observations $\{(x_1, y_2), (x_2, y_3), \dots, (x_{n-1}, y_n)\}$ to estimate the nonlinear model and predict \hat{y}_{n+1} and \bar{y}_{n+1} . We then include the information in the $n + 1$ period and predict \hat{y}_{n+2} and \bar{y}_{n+2} using $\{(x_1, y_2), (x_2, y_3), \dots, (x_n, y_{n+1})\}$. The procedure continues until we obtain \hat{y}_{n+R} and \bar{y}_{n+R} . The predicted values are denoted by:

$$\begin{aligned} &\hat{y}_{n+1}, \hat{y}_{n+2}, \dots, \hat{y}_{n+R} \\ &\bar{y}_{n+1}, \bar{y}_{n+2}, \dots, \bar{y}_{n+R} \end{aligned}$$

Using these predicted values, we can calculate the $R_{OOS,j,n,R}^2$ using the definition (4.3).

To show how the out-of-sample forecasting performance when the forecasting window is expanding, we look at the cumulative out-of-sample R^2 . Cumulative $R_{OOS,n,R}^2$ can be obtained with R ranging from 1 to 124 (the total number of out-of-sample period). In [Cheng et al. \(2019\)](#), they use R_{OOS}^2 starting from $R = 12$ (1 year, 12 months). Therefore in this chapter, I will follow their choice of R_{OOS}^2 and start from $R = 4$ (1 year, 4 quarters).

We report the out-of-sample results against sample mean model in 8 figures (corresponding to 8 functional forms). Each figure contains 4 sub-figures and they show the OOS performances using the 4 co-integrated combinations. We put the R_{OOS}^2 statistics on the vertical axis and the beginning of the various out-of-sample evaluation periods are on the horizontal axis.

Figure (7) and (8) present the performances of the two trigonometric functions compared with sample mean. For the 4 variable pairs, g_1 and g_2 give similar OOS performances and we can only find positive R_{OOS}^2 for combinations co2 (tbl and lty) and co4 (baa or aaa-rated bonds). But from the sub-figure (d), we can see that function g_1 is better than g_2 since it provide consecutive positive R_{OOS}^2 from 1996 to 2012.

Figure (9) and (10) display results for the scaled trigonometric functions g_3 and g_4 . These two functions are different from g_1 and g_2 in that they have a scale parameter in front of the single-index while g_1 and g_2 do not. Similar to the trigonometric functions, g_3 and g_4 only show positive R_{OOS}^2 for combinations co2 (lty and tbl) and co4 (baa or aaa-rated bonds), and most of the positive results are in the early periods of the out-of-sample forecasts. We can also see that g_3 performs better than g_4 as it provides a consecutive R_{OOS}^2 for co4 between 1996 to 2010.

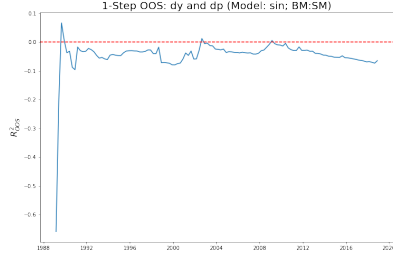
The results for the two exponential functions are presented in figure (11) and (12). For functional g_5 , it cannot outperform sample mean model for most of the out-of-sample forecasting period. We can only find a positive spike around 1992 for co1 (dp and dy), co2 (lty and tbl) and co4 (baa or aaa-rated bonds).

For functional g_6 , the positive R_{OOS}^2 can be found in the first half of the forecasting period. We can see from sub-figures (b) and (d) of figure (12) that g_6 gives consecutive positive results before 2014 when using combinations co2 and co4.

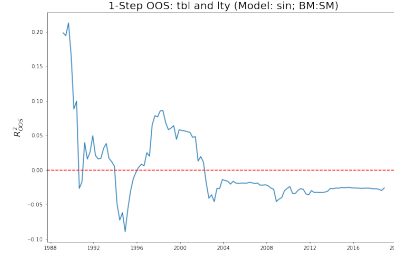
Figure (13) presents the forecasting results of the polynomial function g_7 . Positive R_{OOS}^2 can be found for combinations co2 and co4 before 2014. Forecasting results of g_8

in figure (14) are similar to g_7 for combinations co1, co2 and co3. Although the results of co4 is different, the positive values are only present in the first half of the forecasting period.

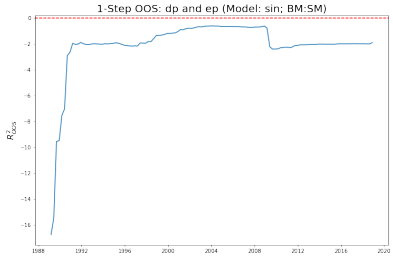
Figure 7: OOS Results for Model with f_1



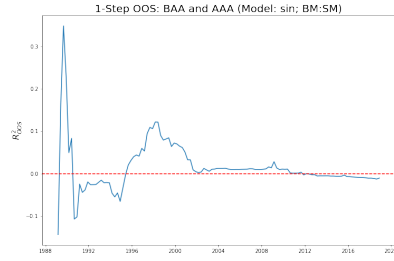
(a) co1



(b) co2

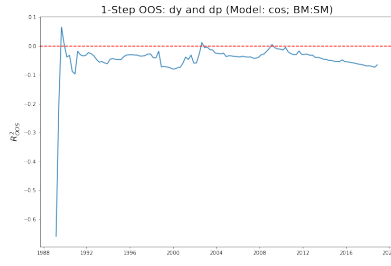


(c) co3

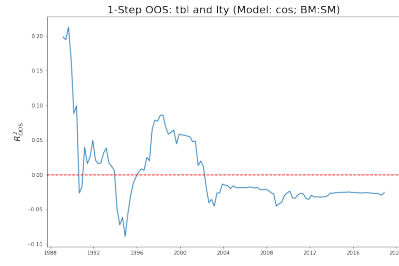


(d) co4

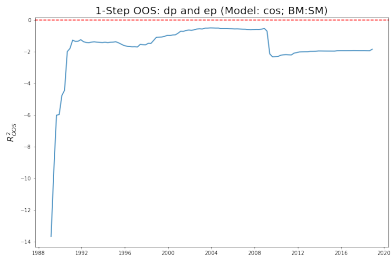
Figure 8: OOS Results for Model with f_2



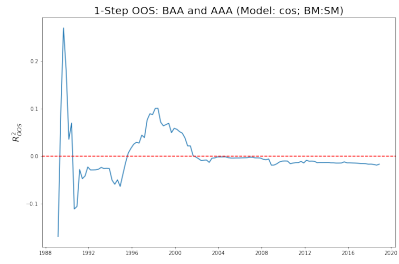
(a) co1



(b) co2

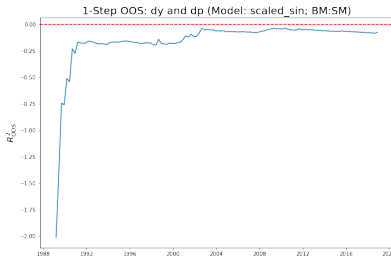


(c) co3

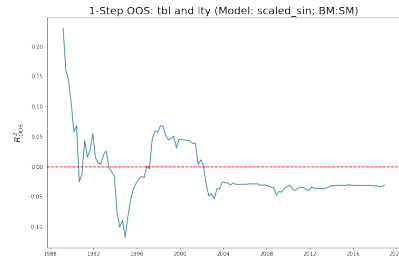


(d) co4

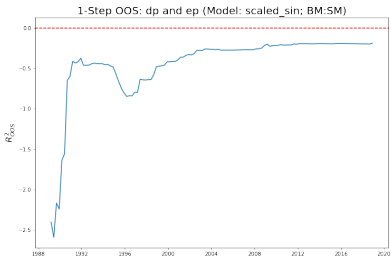
Figure 9: OOS Results for Model with f_3



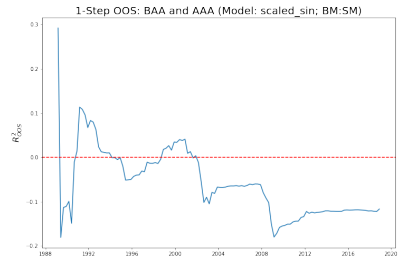
(a) co1



(b) co2

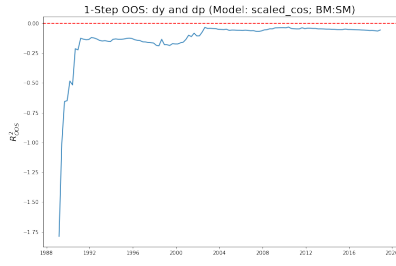


(c) co3

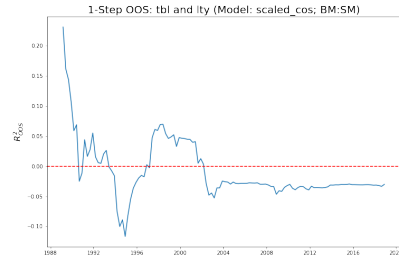


(d) co4

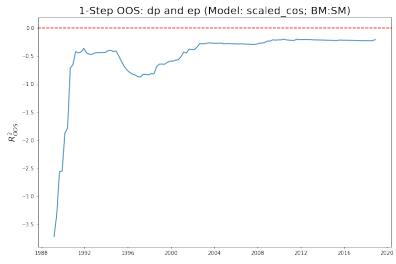
Figure 10: OOS Results for Model with f_4



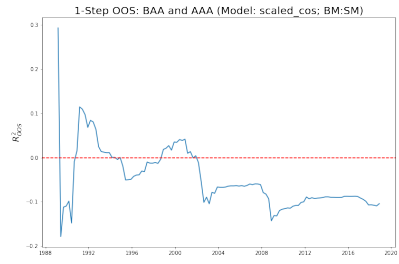
(a) co1



(b) co2

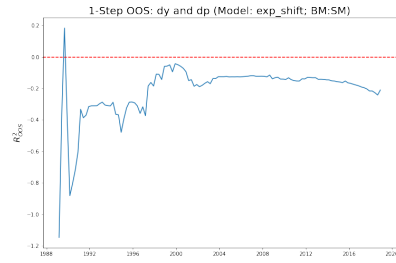


(c) co3

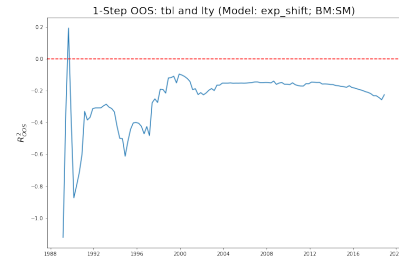


(d) co4

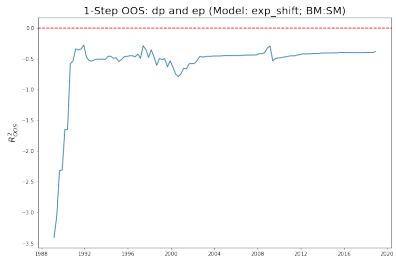
Figure 11: OOS Results for Model with f_5



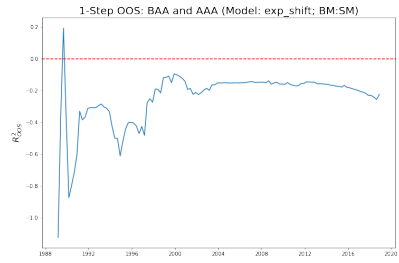
(a) co1



(b) co2

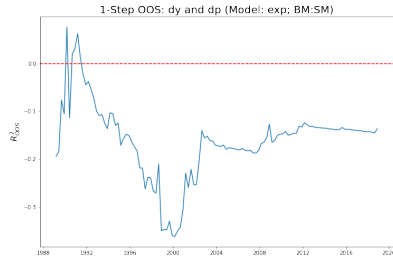


(c) co3

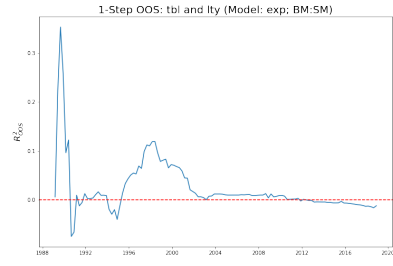


(d) co4

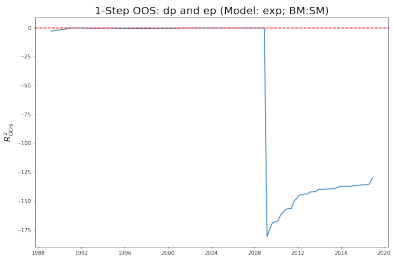
Figure 12: OOS Results for Model with f_6



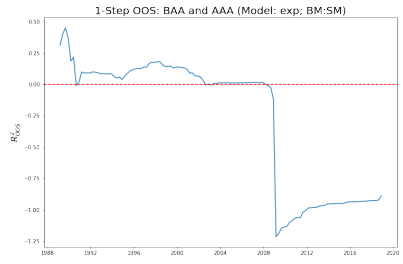
(a) co1



(b) co2

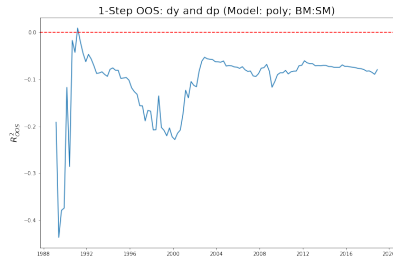


(c) co3

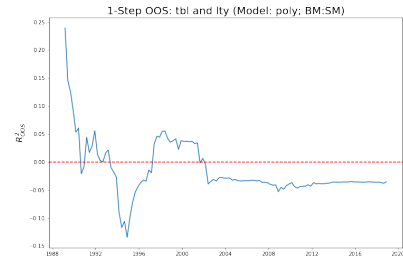


(d) co4

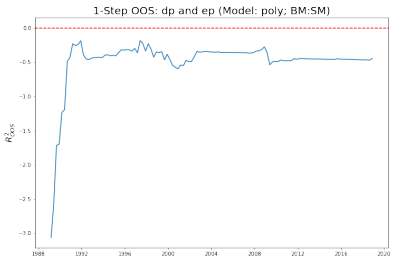
Figure 13: OOS Results for Model with f_7



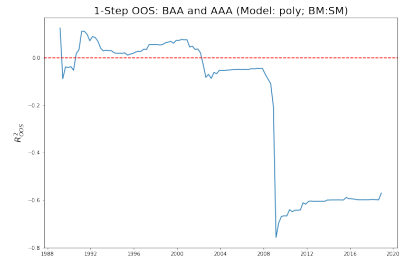
(a) co1



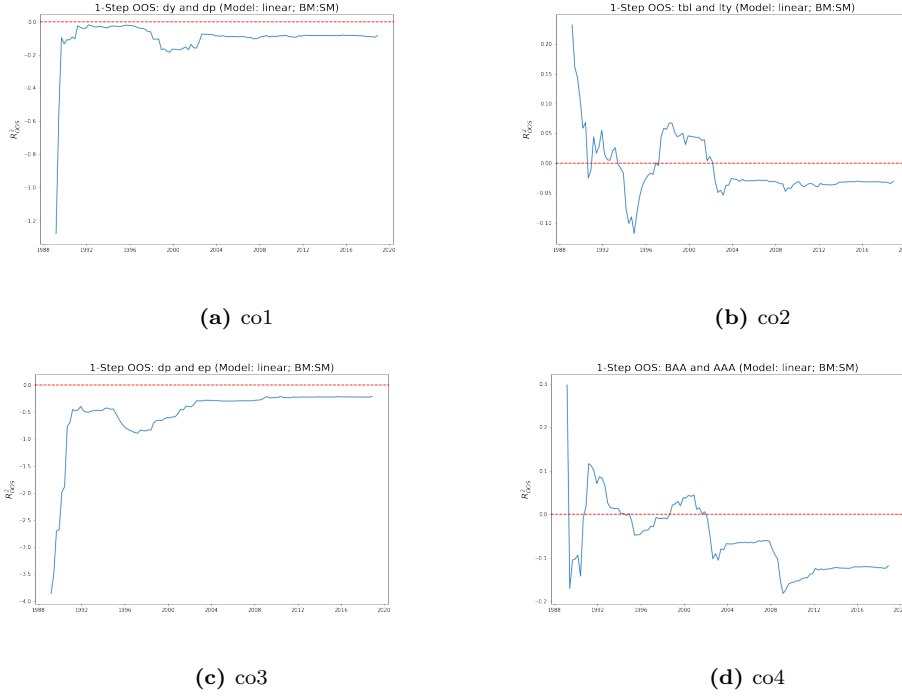
(b) co2



(c) co3



(d) co4

Figure 14: OOS Results for Model with g_8 

To compare the performances of the 8 functional forms with the 4 different variable combinations, we calculate the percentage of positive R_{OOS}^2 in the forecasting period. The results are shown in table (13). It is clear that for combination co3 (dp and ep), none of the functions can perform better than sample mean prediction. However, for combinations co2 and co4, for more than half of out-of-sample period, g_1 and g_6 can outperform sample mean. And other functional forms also can provide positive results.

Table 13: Percentage of Positive R_{OOS}^2

	g_1	g_2	g_3	g_4	g_5	g_6	g_7	g_8
co1	3.23%	3.23%	0.00%	0.00%	2.42%	7.26%	4.03%	0.00%
co2	37.90%	37.90%	32.26%	32.26%	2.42%	68.55%	29.84%	32.26%
co3	0.00%	0.00%	0.00%	0.00%	0.00%	0.00%	0.00%	0.00%
co4	57.26%	24.19%	24.19%	26.61%	2.42%	62.90%	41.94%	27.42%

To conclude, no matter which function we use, combinations co2 and co4 tend to have better results than other variable pairs. And among the 8 functions, g_6 is the best for all

the 4 combinations in terms of the percentage of positive R_{OOS}^2 . The two trigonometric functions also provide good OOS results, especially for g_1 and $co4$. But considering the scale parameter in g_3 and g_4 does not improve the forecast. For polynomial function, it can outperform sample mean except for combination $co3$, although it is not as good as other functional forms.

OOS Performance Compared with Linear Models

Although sample mean is widely used in comparing OOS performance of stock return predictability, there are also other models being studied in previous research. In this section, we will use AR(1) model, AR(2) model and also a linear model with the "cay" variable (see [Lettau and Ludvigson \(2001\)](#)) as benchmarks.

AR model is a widely used time series model (see for example, [Box et al. \(2015\)](#), [Mobarek and Keasey \(2000\)](#) and [Areal and Taylor \(2002\)](#)) and is a representation of a type of random processes. It specifies that the dependent variable depends linearly on its own lagged values. In the model we proposed in this chapter, we also include the previous value of dependent variable as a predictor. In figure 15, we plot the R_{OOS}^2 value when using AR(1) model as the benchmark.

We can see from the two figures that the partially nonlinear models consistently perform better before 2005. When using model containing the Sine function (f_1) and variable combination $co2$ (tbl and lty), our partially nonlinear model can outperform AR(1) model for most of the period before 2006, and the two models have a similar performance between 2006 and 2009. Similar for the model with functional form f_5 , our model also performs better when using $co2$ before 2012.

Figure 16 presents the R_{OOS}^2 value when using AR(2) as the benchmark. When compared with the AR(2) model, the partially nonlinear models also provide a good out-of-sample performance. The model with nonlinear part f_3 outperforms the AR(2) model before 2009 when using variable combination $co4$ (baa and aaa rated bonds). And for the model with nonlinear component f_5 , it outperforms the AR(2) model during the whole out-of-sample period (for variable combination $co2$).

We also consider the AR(1) model with an additional "cay" variable, which has been considered in the study of [Lettau and Ludvigson \(2001\)](#). It is the special case of our

Figure 15: OOS Performance (Benchmark: AR(1) Model)

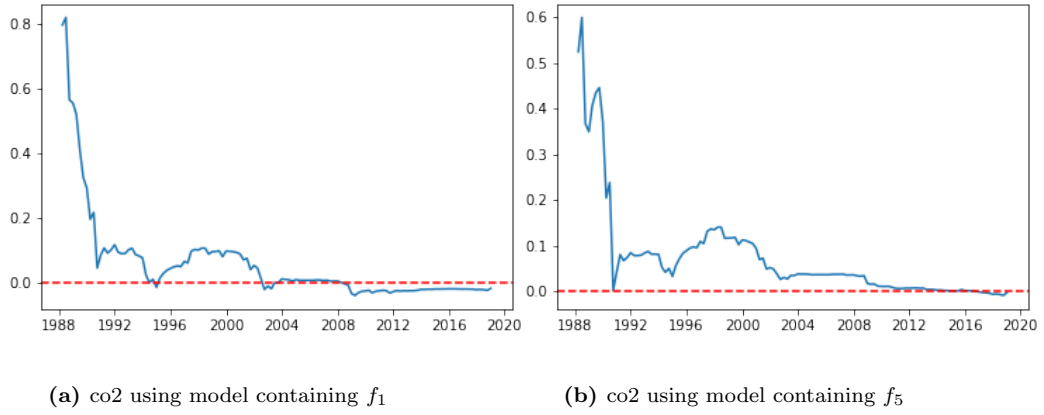
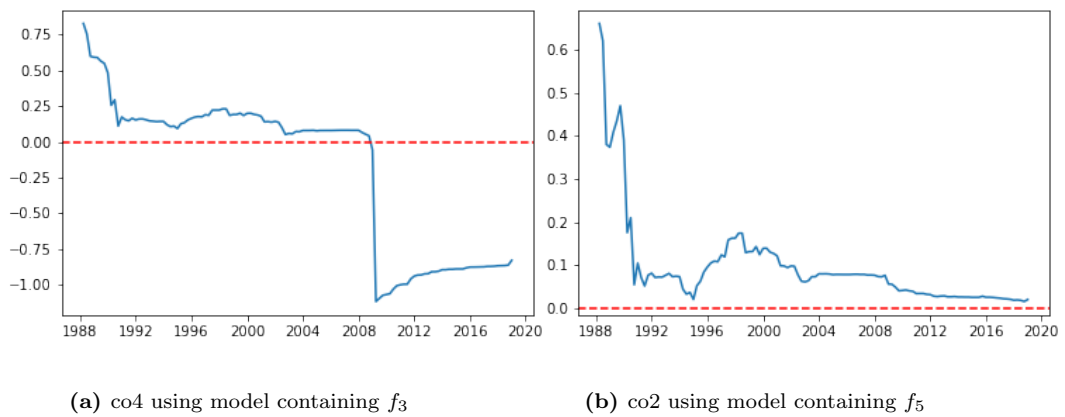


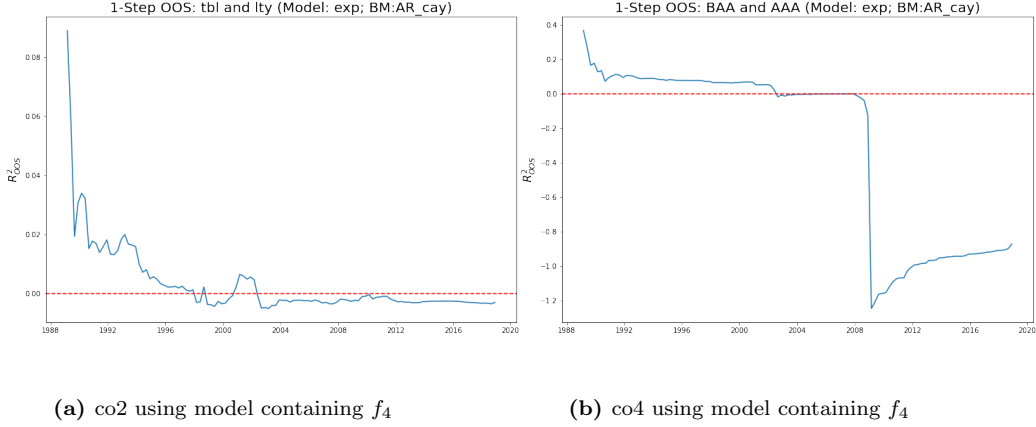
Figure 16: OOS Performance (Benchmark: AR(2) Models)



partially nonlinear model (1.1). When the nonlinear part $f(x'_{t-1}\theta_0; \gamma_0)$ is not significant, model (1.1) become a linear model with only stationary variables.

From figure 17, we can see that when using model containing nonlinear function f_4 with variable combinations co2 and co4, the nonlinear model can outperform the linear model before 2000.

Figure 17: OOS Performance (Benchmark: AR(1) Models with "cay" Variable)



OOS Performance Compared with Nonlinear Models

In our previous chapter, we proposed a nonlinear single-index model of the form:

$$y_t = f(x'_{t-1}\theta, \gamma)$$

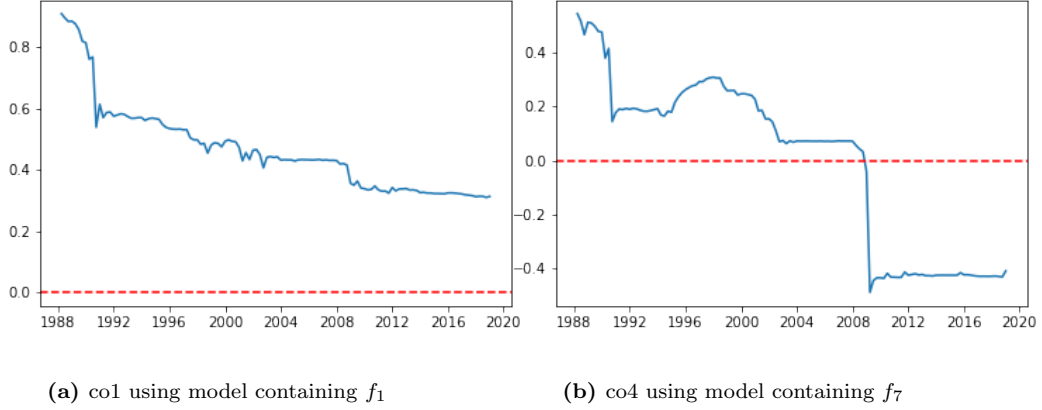
where f take the same 7 forms in this chapter.

Figure 18 presents the R^2_{OOS} when using the nonlinear models in chapter 2 as the benchmark model. In the nonlinear model, we did not include the stationary variables but we considered the same nonlinear functional forms.

From the figure, we can see that when using variable combination co2 and function with nonlinear form f_1 , the partially nonlinear model can outperform the nonlinear model during the whole out-of-sample period. And for the variable combination co4, when using function containing nonlinear part f_7 , the partially nonlinear model outperforms the nonlinear model before 2009.

Therefore, we can conclude that the partially nonlinear models can outperform some commonly used linear models and the nonlinear model we proposed in chapter 2.

Figure 18: OOS Performance (Benchmark: Nonlinear Model)



5 conclusion

In this chapter, we consider a partially nonlinear single-index model, which allows for lagged dependent variables, stationary variables, cointegrated and non-cointegrated variables. We propose a three-step estimation method to estimate the model and includes a constraint on θ (the coefficient for the non-stationary variables) and a truncation condition on x_t .

From the simulation results, we can see that the estimators have good finite sample properties and good convergence. We also find that the constraint provides finite sample gains for the CLS estimators. In addition, we also find that when using cointegrated x_t , both the NLS and CLS estimators have a better performance. And among the 7 functional forms we consider, the model with polynomial functional form gives the best simulation performance.

Based on the simulation results, we focus on cointegrated variables and the constrained nonlinear least square method in the empirical study. We apply the model to the [Welch and Goyal \(2008\)](#) dataset and investigate the predictability using co-integrated variable combinations. We find that the partially nonlinear models can outperform sample mean model both in-sample and out-of-sample. When using other benchmark models, such as AR(1) model and AR(2) model, our models also provides better in-sample performance for certain variable combinations and nonlinear functional forms. In terms of out-of-sample, our models outperforms the two time series models in a consecutive period.

And by including lagged dependent variable and the stationary "cay" variable, the partially nonlinear models give better out-of-sample forecast than the nonlinear models over a consecutive period. Therefore, we can conclude that by considering nonlinearities and auto-correlation in the dependent variable, we can achieve out-of-sample forecasting gains.

Bibliography

- Andrews, D. W. and McDermott, C. J. (1995), ‘Nonlinear econometric models with deterministically trending variables’, *The Review of Economic Studies* **62**(3), 343–360.
- Areal, N. M. and Taylor, S. J. (2002), ‘The realized volatility of ftse-100 futures prices’, *Journal of Futures Markets: Futures, Options, and Other Derivative Products* **22**(7), 627–648.
- Birke, M., Van Bellegem, S. and Van Keilegom, I. (2017), ‘Semi-parametric estimation in a single-index model with endogenous variables’, *Scandinavian Journal of Statistics* **44**(1), 168–191.
- Box, G. E., Jenkins, G. M., Reinsel, G. C. and Ljung, G. M. (2015), *Time series analysis: forecasting and control*, John Wiley & Sons.
- Campbell, J. Y. and Shiller, R. J. (1988), ‘Stock prices, earnings, and expected dividends’, *The Journal of Finance* **43**(3), 661–676.
- Campbell, J. Y. and Thompson, S. B. (2008), ‘Predicting excess stock returns out of sample: Can anything beat the historical average?’, *The Review of Financial Studies* **21**(4), 1509–1531.
- Campbell, J. Y., Vuolteenaho, T. and Ramadorai, T. (2004), ‘Caught on tape: Predicting institutional ownership with order flow’, *Harvard Institute of Economic Research Discussion Paper* (2046).
- Campbell, J. Y. and Yogo, M. (2006), ‘Efficient tests of stock return predictability’, *Journal of financial economics* **81**(1), 27–60.
- Chang, Y. and Park, J. Y. (2003), ‘Index models with integrated time series’, *Journal of Econometrics* **114**(1), 73–106.
- Chang, Y., Park, J. Y. and Phillips, P. C. (2001), ‘Nonlinear econometric models with cointegrated and deterministically trending regressors’, *The Econometrics Journal* **4**(1), 1–36.
- Chen, X. (2007), ‘Large sample sieve estimation of semi-nonparametric models’, *Handbook of econometrics* **6**, 5549–5632.
- Cheng, T., Gao, J. and Linton, O. (2019), ‘Nonparametric predictive regressions for stock return prediction’.

- Cochrane, J. H. (2008), ‘The dog that did not bark: A defense of return predictability’, *The Review of Financial Studies* **21**(4), 1533–1575.
- Dong, C., Gao, J. and Peng, B. (2015), ‘Semiparametric single-index panel data models with cross-sectional dependence’, *Journal of Econometrics* **188**(1), 301–312.
- Dong, C., Gao, J., Tjøstheim, D. et al. (2016), ‘Estimation for single-index and partially linear single-index integrated models’, *The Annals of Statistics* **44**(1), 425–453.
- Fama, E. F. (1981), ‘Stock returns, real activity, inflation, and money’, *The American economic review* **71**(4), 545–565.
- Fama, E. F. (1990), ‘Stock returns, expected returns, and real activity’, *The journal of finance* **45**(4), 1089–1108.
- Fama, E. F. and French, K. R. (1989), ‘Business conditions and expected returns on stocks and bonds’, *Journal of financial economics* **25**(1), 23–49.
- Gao, J. (2007), *Nonlinear time series: semiparametric and nonparametric methods*, CRC Press.
- Gao, J., King, M., Lu, Z. and Tjøstheim, D. (2009), ‘Nonparametric specification testing for nonlinear time series with nonstationarity’, *Econometric Theory* **25**(6), 1869–1892.
- Jennrich, R. I. (1969), ‘Asymptotic properties of non-linear least squares estimators’, *The Annals of Mathematical Statistics* **40**(2), 633–643.
- Kothari, S. P. and Shanken, J. (1997), ‘Book-to-market, dividend yield, and expected market returns: A time-series analysis’, *Journal of Financial economics* **44**(2), 169–203.
- Lettau, M. and Ludvigson, S. (2001), ‘Consumption, aggregate wealth, and expected stock returns’, *the Journal of Finance* **56**(3), 815–849.
- Lettau, M. and Van Nieuwerburgh, S. (2008), ‘Reconciling the return predictability evidence: The review of financial studies: Reconciling the return predictability evidence’, *The Review of Financial Studies* **21**(4), 1607–1652.
- Li, D., Tjøstheim, D., Gao, J. et al. (2016), ‘Estimation in nonlinear regression with harris recurrent markov chains’, *The Annals of Statistics* **44**(5), 1957–1987.
- Ling, S. (2007), ‘Self-weighted and local quasi-maximum likelihood estimators for arma-garch/igarch models’, *Journal of Econometrics* **140**(2), 849–873.
- Ma, S. and Song, P. X.-K. (2015), ‘Varying index coefficient models’, *Journal of the American Statistical Association* **110**(509), 341–356.

- Mobarek, A. and Keasey, K. (2000), Weak-form market efficiency of an emerging market: Evidence from dhaka stock market of bangladesh, *in* ‘ENBS Conference held on Oslo’, pp. 1–30.
- Park, J. Y. (2002), ‘Nonstationary nonlinear heteroskedasticity’, *Journal of econometrics* **110**(2), 383–415.
- Park, J. Y. and Phillips, P. C. (1999), ‘Asymptotics for nonlinear transformations of integrated time series’, *Econometric Theory* **15**(3), 269–298.
- Park, J. Y. and Phillips, P. C. (2000), ‘Nonstationary binary choice’, *Econometrica* **68**(5), 1249–1280.
- Park, J. Y. and Phillips, P. C. (2001), ‘Nonlinear regressions with integrated time series’, *Econometrica* **69**(1), 117–161.
- Pesaran, M. H. and Timmermann, A. (1995), ‘Predictability of stock returns: Robustness and economic significance’, *The Journal of Finance* **50**(4), 1201–1228.
- Pontiff, J. and Schall, L. D. (1998), ‘Book-to-market ratios as predictors of market returns’, *Journal of financial economics* **49**(2), 141–160.
- Qi, M. (1999), ‘Nonlinear predictability of stock returns using financial and economic variables’, *Journal of Business & Economic Statistics* **17**(4), 419–429.
- Welch, I. and Goyal, A. (2008), ‘A comprehensive look at the empirical performance of equity premium prediction’, *The Review of Financial Studies* **21**(4), 1455–1508.
- Wooldridge, J. M. (1994), ‘Estimation and inference for dependent processes’, *Handbook of econometrics* **4**, 2639–2738.
- Wu, C.-F. (1981), ‘Asymptotic theory of nonlinear least squares estimation’, *The Annals of Statistics* **9**(3), 501–513.
- Xia, Y. and Härdle, W. (2006), ‘Semi-parametric estimation of partially linear single-index models’, *Journal of Multivariate Analysis* **97**(5), 1162–1184.
- Yu, Y. and Ruppert, D. (2002), ‘Penalized spline estimation for partially linear single-index models’, *Journal of the American Statistical Association* **97**(460), 1042–1054.
- Zhou, W., Gao, J., Kew, H. and Harris, D. (2018), ‘Semiparametric single-index predictive regression’, *Available at SSRN 3214042*.

Appendix 1 In-sample Estimation Results

Table 14: Full-sample Estimation Results Using Taylor Initials

		θ_1	θ_2	β_1	β_2	γ		
sin_func	co1	-0.699	0.715	-0.600	0.424	0.257		
	co2	-0.775	0.632	0.064	0.399	0.185		
	co3	-0.953	0.302	0.048	2.130	-1.011		
	co4	-0.742	0.670	0.081	0.474	0.236		
cos_func	co1	-0.699	0.715	-0.600	0.424	-1.314		
	co2	-0.775	0.632	0.063	0.398	30.030		
	co3	-0.953	0.302	0.048	2.130	-2.582		
	co4	-0.743	0.670	0.081	0.474	187.161		
scaled_sin_func	co1	0.678	-0.735	-0.139	0.476	9.132	0.333	
	co2	-0.839	0.544	0.069	0.442	0.212	0.615	
	co3	-0.947	0.320	0.100	0.508	0.313	-0.030	
	co4	0.654	-0.756	0.080	0.624	0.295	4.164	
scaled_cos_func	co1	-0.785	0.619	0.182	0.515	1.247	0.137	
	co2	-0.843	0.538	0.069	0.442	-1.359	0.610	
	co3	-0.932	0.361	0.099	0.507	1.261	0.031	
	co4	-0.654	0.756	0.080	0.624	5.007	-4.178	
exp_func	co1	-0.703	0.711	0.221	0.488	0.219	-8.759	
	co2	-0.662	0.750	0.076	0.127	0.062	-248.540	
	co3	-0.977	0.212	0.099	0.509	0.276	0.018	
	co4	-0.690	0.724	0.092	0.473	0.218	-518.196	
exp_shift_func	co1	-0.577	-0.817	0.101	2.228	-5.264	-0.166	
	co2	-0.835	-0.550	0.101	2.228	-8.194E+09	-1.162E+11	
	co3	-0.913	0.408	0.101	-0.003	2.293	-0.097	
	co4	-0.678	0.735	0.101	2.228	19.311	-0.418	
poly_func	co1	-0.712	0.702	2.089	0.622	0.388	-2.940	2.204
	co2	-0.696	0.718	0.068	0.382	0.168	2.277	-61.876
	co3	-0.910	0.415	0.105	0.471	0.646	-0.379	0.082
	co4	-0.661	0.751	0.056	0.708	0.326	-6.473	-372.950
linear_func	co1	-0.713	0.702	2.049	0.643	0.412	-2.792	
	co2	-0.841	0.542	0.069	0.443	0.210	0.600	
	co3	-0.950	0.313	0.099	0.508	0.308	-0.028	
	co4	-0.654	0.757	0.080	0.619	0.288	-3.938	